Allosteric activation of exopolysaccharide synthesis through cyclic di-GMP-stimulated protein-protein interaction

Samuel Steiner[1], Christian Lori[1], Alex Boehm[2] and Urs Jenal[1]

Affiliations:

[1] Biozentrum, University of Basel, Klingelbergstrasse 50/70, CH-4056 Basel, Switzerland

[2] LOEWE-Zentrum für Synthetische Mikrobiologie, Philipps-Universität Marburg, Hans-Meerwein-Strasse 6, D-35043 Marburg, Germany

Running title: C-di-GMP-activated poly-GlcNAc synthesis

Final character count: 57'400 (including spaces)

For correspondence: urs.jenal@unibas.ch

Abstract

In many bacterial pathogens the second messenger c-di-GMP stimulates the production of an exopolysaccharide (EPS) matrix to shield bacteria from assaults of the immune system. How c-di-GMP induces EPS biogenesis is largely unknown. Here we show that c-di-GMP allosterically activates the synthesis of poly-β-1,6-*N*-acetylglucosamine (poly-GlcNAc), a major extracellular matrix component of *Escherichia coli* biofilms. C-di-GMP binds directly to both PgaC and PgaD, the two inner membrane components of the poly-GlcNAc synthesis machinery to stimulate their glycosyltransferase activity. We demonstrate that the PgaCD machinery is a novel type c-di-GMP receptor, where ligand binding to two proteins stabilizes their interaction and promotes enzyme activity. This is the first example of a c-di-GMP-mediated process that relies on protein-protein interaction. At low c-di-GMP concentrations PgaD fails to interact with PgaC and is rapidly degraded. Thus, when cells experience a c-di-GMP trough, PgaD turnover facilitates the irreversible inactivation of the Pga machinery, thereby temporarily uncoupling it from c-di-GMP signaling. These data uncover the mechanism of c-di-GMP-mediated EPS control and provide a frame for c-di-GMP signaling specificity in pathogenic bacteria.

Keywords: biofilm/c-di-GMP/glycosyltransferase/poly-GlcNAc/signaling

Introduction

Most bacteria are able to switch from a motile planktonic 'lifestyle' to growth in surface-associated multicellular communities known as biofilms. Within these structures, cells are encased in a self-produced extracellular polymeric matrix that is typically composed of proteinaceous adhesin factors, DNA and exopolysaccharides (EPS) (Branda *et al*, 2005; Flemming and Wingender, 2010). This complex biofilm structure is known to protect bacteria from antimicrobials, physical stresses and the predation by the host immune system. Bacterial biofilms are often associated with chronic infections and infection relapses causing health problems of growing importance (Costerton *et al*, 1999; Mah and O'Toole, 2001; Davies, 2003; Hall-Stoodley *et al*, 2004; Fux *et al*, 2005).

The second messenger bis-(3'-5')-cyclic dimeric GMP (c-di-GMP) plays a central role in integrating environmental and cellular cues to control this major bacterial 'lifestyle' transition by disfavoring single cell behavior and by promoting biofilm formation. C-di-GMP is synthesized from GTP by diguanylate cyclases (DGCs) that harbor a conserved GGDEF domain (Paul *et al*, 2004) and is degraded to the linear dinucleotide pGpG by specific phosphodiesterases (PDEs) that harbor either a conserved EAL (Christen *et al*, 2005) or HD-GYP domain (Ryan *et al*, 2006; Hengge, 2009; Schirmer and Jenal, 2009). While DGCs and PDEs have been analyzed in detail, both structurally and functionally, little is known about how c-di-GMP acts on downstream targets. Only a few c-di-GMP-specific receptor protein families have been described up to now, for most of which mechanistic details are lacking (Sondermann *et al*, 2011) (Lee 2007; Merighi 2007; Christen 2007; Duerig 2009; Newell 2011).

In *Escherichia coli*, c-di-GMP regulates several cellular processes including EPS production, the biogenesis of fimbriae, flagellar-based motility and RNA degradation (Pesavento *et al*, 2008; Monteiro *et al*, 2009; Boehm *et al*, 2009; Tagliabue *et al*, 2010; Boehm *et al*, 2010; Paul *et al*, 2010; Fang and Gomelsky, 2010; Tuckerman *et al*, 2011; Povolotsky and Hengge, 2012). To colonize surfaces, *E. coli* produces the EPS poly-β-1,6-*N*-acetylglucosamine (poly-GlcNAc) (Wang *et al*, 2004). This linear homopolymer was implicated in biofilm formation in a wide variety of pathogenic bacteria including *Staphylococcus* spp. and *Yersinia pestis*, where it can promote virulence and contribute to survival in the animal host (Maira-Litrán *et al*, 2005; O'Gara, 2007; Cerca *et al*, 2007; Izano *et al*, 2007, 2008; Bobrov *et al*, 2008; Choi *et al*, 2009; Becker *et al*, 2009; Conover *et al*, 2010; Pérez-Mendoza *et al*, 2011; Yakandawala *et al*, 2011; Bentancor *et al*, 2012; Skurnik *et al*, 2012).

In *E. coli*, poly-GlcNAc is synthesized and secreted by the envelope-spanning Pga machinery (Figure 1A), which is encoded by the *pgaABCD* operon (Wang *et al*, 2004). While PgaA and PgaB

are required for poly-GlcNAc export, PgaC and PgaD are necessary for poly-GlcNAc synthesis (Figure 1A) (Itoh *et al*, 2008). PgaA is an outer membrane porin that serves to translocate growing poly-GlcNAc chains to the cell surface (Itoh *et al*, 2008). PgaB is a putative outer membrane lipoprotein that deacetylates about 3% of the GlcNAc residues during poly-GlcNAc export (Wang *et al*, 2004; Itoh *et al*, 2008). PgaC is a processive β-glycosyltransferase (GT) of the GT-2 family that is located in the inner membrane and polymerizes poly-GlcNAc from activated UDP-GlcNAc precursor (Saxena and Brown, 1997; Wang *et al*, 2004; Itoh *et al*, 2008). The catalytic domain of GT-2 family members is exposed to the cytoplasm (Heldermon *et al*, 2001; Ciocchini *et al*, 2006; Bobrov *et al*, 2008) with sugar transfer through the cytoplasmic membrane being independent of an undecaprenyl phosphate lipid carrier (Gerke *et al*, 1998). Finally, PgaD is a small protein with two predicted N-terminal transmembrane helices. Its function is unknown and it does not show any obvious similarity to other protein families or domains. However, because PgaD is essential for poly-GlcNAc synthesis (Wang *et al*, 2004), it was suggested to assist the GT in polymerizing poly-GlcNAc (Itoh *et al*, 2008).

The expression of the *E. coli pgaABCD* operon is tightly regulated on multiple levels. Most importantly, *pgaABCD* translation is repressed by the action of the RNA binding protein CsrA (carbon storage regulator A) (Wang *et al*, 2005). This global regulator antagonistically controls numerous cellular pathways. E.g., it promotes motility, glycolysis and virulence, while repressing EPS production and gluconeogenesis (Romeo *et al*, 1993; Suzuki *et al*, 2006; Timmermans and Van Melderen, 2010; Romeo *et al*, 2012). In addition, CsrA inhibits the expression of *ydeH* and *ycdT*, two genes encoding DGCs (Jonas *et al*, 2008). The observation that YdeH stimulates poly-GlcNAc-dependent biofilm formation (Boehm *et al*, 2009) argued that the expression of this DGC and its target, the Pga machinery, is coupled via CsrA. YdeH and c-di-GMP were shown to control poly-GlcNAc biogenesis on a post-transcriptional level (Boehm *et al*, 2009), but the mechanism responsible for this induction is unknown.

In this paper, we unravel a novel allosteric mechanism through which c-di-GMP stimulates poly-GlcNAc-dependent biofilm formation in *E. coli*. We show that c-di-GMP allosterically activates the PgaCD GT complex. We present genetic and biochemical evidence arguing that c-di-GMP binds to both inner membrane components of the Pga machinery, thereby mediating their productive interaction and the formation of an active GT complex. Finally, we demonstrate that in the absence of c-di-GMP PgaD is rapidly degraded, offering the means to shut-off the Pga machinery in response to c-di-GMP fluctuations and to temporarily uncouple it from c-di-GMP signaling in the absence of *de novo* synthesis of Pga components. These studies offer a molecular

frame for the widespread c-di-GMP-based activation of bacterial EPS systems and provide the basis for signaling specificity of c-di-GMP-controlled systems.

Results

PgaD *in vivo* stability depends on c-di-GMP

We have previously shown that PgaD steady state protein levels are positively controlled by c-di-GMP on a post-transcriptional level (Boehm *et al*, 2009). This observation was used as an entry point to address the molecular mechanism of c-di-GMP-regulated poly-GlcNAc biogenesis. To mimic the induced state of the Csr regulon, all assays were done in a partial loss-of-function *csrA*::Tn*5* mutant strain background (Romeo *et al*, 1993), which will be referred to as control strain throughout this work. In order to monitor all Pga complex components individually, 3xFlag-tagged versions of PgaA, PgaB, PgaC and PgaD were constructed. In the absence of the DGC YdeH the protein levels of PgaD were reduced, while the levels of the other three Pga proteins remained constant, regardless of whether the *pga* operon was expressed from its native promoter with the 5′ UTR of *pgaA* or from the L-arabinose-dependent P_{ara} promoter with the 5′ UTR of *araB* (Figure 1B and Supplementary Figure 1A). Moreover, PgaD levels were strongly reduced in a Δ*pgaC* mutant, but were restored in a c-di-GMP-dependent manner when *pgaC* was expressed *in trans* and were further increased upon overexpression of *pgaC* (Figure 1C). PgaD levels were still c-di-GMP-dependent in cells expressing a *pgaC* active site mutant (D256N), arguing that PgaC protein but not PgaC glycosyltransferase activity is required to stabilize PgaD (Supplementary Figure 1B). Finally, expression of the heterologous DGC *dgcA* (Christen *et al*, 2006) strongly elevated PgaD levels in a Δ*ydeH* mutant, but only when *pgaC* was present (Supplementary Figure 1C).

The above data indicated that PgaC and c-di-GMP together control PgaD levels post-translationally. To substantiate this and to demonstrate that the effect is specific for PgaD, *pgaD* was replaced with *yfiR*, an unrelated gene from *Pseudomonas aeruginosa*. The observation that YfiR levels failed to fluctuate in response to c-di-GMP availability excludes the possibility that PgaD levels respond to a c-di-GMP-controlled promoter or to translation initiation control elements within *pgaABC* (Supplementary Figure 1D). Next, *in vivo* protein stability of PgaD-3xFlag was determined under different c-di-GMP concentrations upon blocking *de novo* protein biosynthesis in exponentially growing cells. While PgaD remained stable over time in strains with normal or increased c-di-GMP levels (control strain and Δ*ydeH* mutant expressing *dgcA*), the protein was rapidly degraded in strains with low cellular c-di-GMP concentrations (Δ*ydeH* mutant

and Δ*ydeH* mutant expressing an active site mutant of *dgcA*) (Figure 1D and Supplementary Figure 1E).

In summary, these data suggest that c-di-GMP positively modulates PgaD protein stability in a PgaC-dependent manner.

C-di-GMP and PgaD together promote poly-GlcNAc-dependent biofilm formation

The *E. coli csrA*::Tn*5* mutant strain (control strain) forms biofilms under laboratory conditions that fully depend on the EPS adhesin poly-GlcNAc (Wang *et al*, 2004). To test if c-di-GMP is essential for poly-GlcNAc-dependent biofilm formation, multiple genes coding for potential DGCs (each containing a GGDEF domain) were successively deleted. Concomitant deletions of the two CsrA-controlled genes *ydeH* and *ycdT* (Jonas *et al*, 2008) resulted in a drastic reduction of biofilm formation, while a strain carrying a total of seven deletions (*ydeH*, *ycdT*, *yegE*, *yfiN*, *yhjK*, *ydaM*, *yneF*) completely lost the ability to form biofilms (Figure 1E). This strain showed a strongly reduced cellular c-di-GMP level in comparison to the control strain (Figure 1E) and will be referred to as Δ7 strain throughout this work. Importantly, both biofilm deficiency and c-di-GMP level could be complemented by reintroducing only *ydeH* into the bacterial genome (Figure 1E), supporting the idea that YdeH represents the major DGC responsible for poly-GlcNAc induction under these conditions (Boehm *et al*, 2009). In line with the data described above, PgaD protein was not detectable in the Δ7 mutant (Figure 1E). While c-di-GMP is required for normal PgaD levels under physiological conditions, overexpression of *pgaD* resulted in a biofilm induction both in the presence and in the absence of YdeH (Supplementary Figure 1F). However, the Δ*ydeH* mutant never reached the same level of biofilm formation as the control strain, arguing that PgaD and c-di-GMP are synergistically needed for optimal biofilm formation.

C-di-GMP enhances PgaC-PgaD interaction

One scenario that could explain PgaC-dependent PgaD stability is a direct interaction of the two membrane proteins. Co-immunoprecipitation experiments using detergent-solubilized membranes revealed that PgaC and PgaD indeed form a stable complex that was resistant to high salt concentrations and up to 2 M urea (Figure 2A). When overexpressed, PgaC and PgaD could be co-purified even from membranes of a Δ7 strain (Figure 2B), arguing that under these conditions c-di-GMP is no longer required for PgaD stability. Together, this suggested that PgaC and PgaD form a stable complex in the cytoplasmic membrane, the formation of which is mediated by c-di-GMP under physiological conditions.

To test if c-di-GMP is involved in PgaC-PgaD interaction, a bacterial two-hybrid (BacTH) assay was used that is based on the interaction-mediated reconstitution of the split cAMP signaling pathway in *E. coli* (Karimova *et al*, 1998). In this assay, full-length PgaC and PgaD showed a robust interaction (Figure 2C), while all truncated variants (e.g. predicted cytosolic parts) were negative (Supplementary Table 2). The interaction was stimulated by the ectopic expression of the heterologous DGC *dgcA* (Figure 2D and Supplementary Figure 2). Conversely, a step-wise reduction of the cellular c-di-GMP pool gradually lowered the interaction strength. PgaC-PgaD interaction was weakened upon deletion of *ydeH* and abolished in the Δ7 strain (Figure 2D and Supplementary Figure 2). These data further support the idea that c-di-GMP stimulates PgaC-PgaD interaction or complex stability.

The above results can be interpreted in two different ways. C-di-GMP could regulate poly-GlcNAc production by determining PgaD stability and availability. Alternatively, c-di-GMP could promote PgaC-PgaD interaction with PgaD instability and degradation being a consequence of complex disintegration at low c-di-GMP concentrations. To be able to distinguish between these two possibilities, PgaD was 'stabilized' under low c-di-GMP conditions by directly fusing its N-terminus to the C-terminus of PgaC. Surprisingly, the resulting *pgaCD* fusion construct (*pgaCD*f) was fully functional and able to complement biofilm formation of a Δ*pgaCD* mutant in a c-di-GMP-dependent manner (Figure 2E). But in contrast to PgaD, the level of the PgaCD fusion protein (PgaCDf) was unaltered in a strain with lower c-di-GMP concentrations (Figure 2E). These findings reinforce the notion of a direct interplay between PgaC and PgaD and imply that PgaD instability at low c-di-GMP levels is not the cause for Pga control, but may simply result from weak protein interactions under these conditions. These data raise the question why the homologues of PgaC and PgaD exist as two separate proteins in all bacteria harboring this EPS biogenesis system (see below).

C-di-GMP acts as an allosteric activator of PgaCD glycosyltransferase activity

In order to test whether c-di-GMP acts as an allosteric activator for the PgaCD GT complex, an *in vitro* activity assay was developed with membranes containing PgaCD. GT activity was determined indirectly using a modified enzyme-coupled spectrophotometric assay (Baykov *et al*, 1988) or directly by measuring UDP-GlcNAc consumption. In agreement with earlier data demonstrating that both PgaC and PgaD are needed for poly-GlcNAc synthesis *in vivo* (Wang *et al*, 2004; Itoh *et al*, 2008), UDP-GlcNAc was only turned over to poly-GlcNAc and UDP by membranes of cells expressing *pgaC* and *pgaD* (Figure 3A). Following incubation of active membranes with substrate for several hours, a slimy and viscous reaction product was visualized by light microscopy (Figure

3B). Immunoblot analysis with an anti-poly-GlcNAc antibody confirmed the identity of the reaction product (Supplementary Figure 3A). Experiments to determine the substrate affinity of the PgaCD GT complex revealed a K_m for UDP-GlcNAc of 270.5 ± 37.2 μM (Figure 3C). To test if PgaCD GT activity is stimulated by c-di-GMP, initial reaction velocities were measured at varying c-di-GMP concentrations in the presence of a constant UDP-GlcNAc concentration of 50 μM. Under these conditions, c-di-GMP stimulated GT activity more than 20-fold and curve fitting indicated a c-di-GMP concentration for half-maximal initial velocity (K_{act}) of 62.2 ± 7.2 nM (Figure 3D). This induction was highly specific as the addition of GTP failed to activate the enzyme and furthermore, the c-di-GMP-mediated activity was fully dependent on the PgaCD machinery (Supplementary Figure 3B). The basal enzymatic GT activity in the absence of exogenously added c-di-GMP correlated with the cellular c-di-GMP concentration of the strain used for *pgaCD* overexpression and membrane preparation. Almost no basal activity was detected for membranes originating from the Δ7 mutant (Supplementary Figure 3B). A Lineweaver-Burk plot analysis integrating initial reaction velocity data at different UDP-GlcNAc concentrations in the presence of a non-saturating and a saturating c-di-GMP concentration resulted in fitted lines converging close to the x-axis, indicating that c-di-GMP affects the V_{max} rather than the K_m of the enzyme complex (Figure 3E).

In summary, these data strongly suggest that c-di-GMP acts as a direct allosteric activator of the PgaCD glycosyltransferase complex.

Concomitant binding of c-di-GMP to both PgaC and PgaD

The above *in vitro* assays argued for a direct role of c-di-GMP as an allosteric activator of PgaCD GT activity. To corroborate these findings, c-di-GMP binding to the PgaCD complex was tested by using a c-di-GMP capture compound (cdG-CC). This molecule consists of a c-di-GMP moiety that is asymmetrically modified at the 2′ hydroxyl of one ribose with a linker connecting to a photo-reactive and a biotin sorting group (Nesper *et al*, 2012). The PgaCD complex was specifically and competitively captured by the cdG-CC from membrane preparations (Figure 4A). An excess of c-di-GMP, but not GTP, gradually competed with cdG-CC binding. While the PgaCD complex and the PgaCD fusion protein were specifically pulled-down, no specific binding was observed when membranes were used that only contained PgaC or PgaD (Figure 4B). Although some residual binding to the cdG-CC was observed under these conditions, the addition of an excess of c-di-GMP failed to compete with this interaction (Figure 4B). When membranes were used that contained 3xFlag-tagged variants of both PgaC and PgaD, both proteins showed specific cdG-CC binding. A fraction of the PgaC-PgaD heterodimers withstood boiling in SDS sample buffer and

appeared as a distinct band on the immunoblot, emphasizing the remarkable stability of these complexes (Figure 4B). Probing cdG-CC samples with an antibody against the biotin moiety of the capture compound revealed that the cdG-CC was covalently crosslinked to both PgaC and PgaD in a competitive way, suggesting that c-di-GMP is able to directly interact with both components of the complex (Supplementary Figures 4A and 4B).

To corroborate these findings, UV light-induced crosslinking experiments with radiolabeled c-di-GMP were performed (Christen *et al*, 2006). In good agreement with the data obtained with the capture compound, PgaC and PgaD were specifically and competitively labeled with [^{33}P]c-di-GMP when both proteins were present in the membrane fraction (Figure 4C). An excess of c-di-GMP, but not GTP, efficiently outcompeted the [^{33}P]c-di-GMP crosslink to both proteins. It is interesting to note that PgaC labeling was generally much stronger than PgaD labeling. Again, specific c-di-GMP binding and radiolabeling was only observed in membranes containing both proteins, but was lost for PgaC when PgaD was not present (Figure 4D). Interestingly, the presence of the substrate UDP-GlcNAc increased the specific binding of c-di-GMP, indicating some form of communication between the GT active site and the allosteric c-di-GMP binding pocket within the PgaCD complex (Supplementary Figures 4C and 4D).

Altogether, these data suggest that the PgaCD GT complex represents a novel type c-di-GMP receptor, where ligand binding to two individual proteins promotes their stable interaction and subsequent activation.

Constitutive mutations in *pgaD* uncouple PgaCD activity from c-di-GMP

To more closely define the c-di-GMP binding site in PgaD, variants with C-terminal truncations were analyzed for their ability to stimulate biofilm formation. Although biofilm formation gradually decreased with deletions extending towards the second transmembrane helix, c-di-GMP stimulation was sustained in truncations extending to amino acid R78 (Figures 5A and 5B). This argued that c-di-GMP binds to a region within the first 78 amino acids of PgaD consisting of only two transmembrane helices with short flanking regions in the cytoplasm, thus suggesting that c-di-GMP modulates the interaction of PgaC and PgaD in the vicinity of the cytoplasmic membrane. To test this hypothesis we set up a genetic screen to isolate mutations in *pgaC* and *pgaD* that facilitate biofilm formation in the absence of c-di-GMP. Error-prone PCR mutagenesis and screening for biofilm-forming colonies in the Δ7 strain using Congo Red agar plates led to the isolation of several constitutive mutants (Supplementary Table 3). With one exception, all mutations in PgaD clustered within a short conserved region between the second transmembrane helix and residue R78 (Figure 5A). Two of the activating *pgaD* alleles (N75D,K76E and

L73Q,K76E,R78C) firmly locked biofilm formation at an intermediate level independently of the availability of c-di-GMP (Figure 5C). In both cases this constitutive phenotype required the presence of multiple mutations with single changes showing no or little effect (Figure 5C). While the N75D,K76E mutant completely failed to respond to c-di-GMP, the L73Q,K76E,R78C allele retained some residual induction upon ectopic expression of a heterologous DGC (Supplementary Figure 5A). Interestingly, protein levels of both constitutive PgaD mutants were increased in the Δ7 strain, but in contrast to wild-type PgaD they showed no significant response to changes in cellular c-di-GMP concentration (Figure 5D). The stability of these mutant forms was still dependent on the presence of PgaC (data not shown).

Next, the behavior of the PgaD mutant forms was assayed in the *in vitro* GT activity assay. To avoid possible stoichiometry problems arising from different overall levels of PgaD, assays were performed with normalized protein levels of the PgaCD fusion protein (Supplementary Figure 5B). Both mutant proteins showed a more than 3-fold increased basal GT activity in the absence of exogenously added c-di-GMP and could not be stimulated further by the addition of 100 nM c-di-GMP, a concentration that causes approximately half-maximal activation of the wild-type enzyme (Figures 5E and 3D). These data suggested that constitutive PgaD mutants are able to interact with and stimulate PgaC in the absence of c-di-GMP, thereby uncoupling the PgaCD complex from c-di-GMP signaling. To test if these mutants still bind the allosteric ligand *in vitro*, cdG-CC experiments were performed in the context of the PgaCD fusion protein. Consistent with the data described above, the N75D,K76E mutant almost completely failed to bind the cdG-CC, while the pull-down of the L73Q,K76E,R78C mutant was severely reduced (Figure 5F). These experiments demonstrate that specific mutations in the conserved region of PgaD abolish c-di-GMP binding and at the same time mimic a c-di-GMP-bound state that activates the PgaCD GT complex.

Two conserved residues of PgaD located within the same region, W71 and Y74, were previously shown to be important for the function of the PgaD homologue of *Y. pestis* (Forman *et al*, 2006). While the Y74A mutation did not affect *E. coli* PgaD function, the W71A mutation resulted in an almost complete loss of biofilm formation (Figure 5C). Importantly, while W71 was not required for cdG-CC binding (Figure 5F), the W71A mutation was dominant over the constitutive allele N75D,K76E (Supplementary Figure 5C). This argues that W71 resides downstream of the c-di-GMP-mediated activation in the PgaD signal transduction process.

Constitutive mutations in *pgaC* influence PgaD protein levels

In contrast to the constitutive *pgaD* mutants, all activating mutations isolated in *pgaC* retained some level of c-di-GMP stimulation (Figure 6A and Supplementary Table 3). Moreover, they all still

depended on the presence of PgaD for biofilm formation (data not shown). In case of the *pgaC* S7P,M44T,W60R allele, the combination of three mutations contributes to the high level of biofilm formation in a Δ7 strain (Figure 6A). In contrast, the single mutation V227L strongly upregulated biofilm formation both in the Δ7 strain and in a strain expressing diguanylate cyclases (Figure 6A). Co-expression of the *pgaC* V227L allele with the constitutive *pgaD* N75D,K76E mutant increased biofilm formation up to the fully induced level observed for the V227L single mutant, even when c-di-GMP was absent (Supplementary Figure 6A). These data indicate that PgaC V227L partially uncouples PgaCD GT activity from c-di-GMP, while the PgaD mutant N75D,K76E has a strong dominant effect that fully releases the PgaCD complex from its c-di-GMP dependency. Because PgaC and c-di-GMP are required for PgaD stability *in vivo* (see above), we hypothesized that constitutive *pgaC* mutants should lead to enhanced PgaD levels in the absence of c-di-GMP. As shown in Figure 6B, PgaD was markedly stabilized in Δ7 strains expressing either the triple *pgaC* mutant S7P,M44T,W60R or the single V227L allele. This further substantiates the idea that c-di-GMP stimulation primarily affects PgaC-PgaD interaction, while PgaD stability is merely a consequence of the allosteric control of the Pga machinery.

R222 of PgaC plays an essential role in c-di-GMP-dependent PgaCD activation

In order to identify regions of PgaC involved in c-di-GMP binding, we focused on arginines as they were shown to play a critical role in c-di-GMP binding (Benach *et al*, 2007; Habazettl *et al*, 2011). To identify conserved arginines potentially involved in c-di-GMP binding, PgaC sequences from gram-negative bacteria harboring genes encoding GGDEF and EAL domain proteins were compared to PgaC sequences from gram-negative organisms lacking c-di-GMP (no GGDEF domain proteins) (Supplementary Figure 6D). Based on this analysis, the following six residues, which are only conserved in species with GGDEF domains, were selected and changed to alanines individually or in combination: R56, R58, R133, R222, R428 and R430. Two alleles, R222A and R428A,R430A, were identified that produced normal protein levels *in vivo* (Supplementary Figure 6B), but almost completely failed to support biofilm formation (Figure 6C). The R222A but not the R428A,R430A mutant also showed a strong binding defect for the cdG-CC (Figure 6D). In agreement with a specific role for R222 in c-di-GMP binding, cells expressing the *pgaC* R222A allele were unable to stabilize PgaD. In contrast, PgaD was stabilized by the PgaC GT active site mutant (D256N) in a c-di-GMP-dependent manner (Supplementary Figure 6C). Most importantly, when co-expressed with the constitutive *pgaD* allele N75D,K76E, the PgaC R222A function was restored (Figure 6E). This underscores the tight interplay between PgaC and PgaD and

demonstrates that the R222A mutation does not cause a general loss of PgaC activity, but rather specifically affects c-di-GMP binding and GT activation.

Together, these data suggested a critical role for R222 of PgaC in the c-di-GMP-dependent activation of the PgaCD GT complex and implied that R222 is directly involved in c-di-GMP binding. To test this, UV light-induced crosslinking experiments with radiolabeled c-di-GMP were performed. As shown in Figure 7, both PgaC and PgaD specifically and competitively incorporated radiolabeled c-di-GMP when present in wild-type GT complexes. In contrast, GT complexes containing either PgaD N75D,K76E or PgaC R222A were strongly impaired in c-di-GMP binding. In both cases, the total amount of crosslinked [^{32}P]c-di-GMP was reduced in PgaC as well as in PgaD (Figures 7A and 7B and Supplementary Figure 7), arguing that individual binding mutations in PgaC or PgaD affect the overall binding of the complex. This is consistent with the observation that cdG-CC binding to the PgaCD complex was strongly reduced for the PgaD N75D,K76E and the PgaC R222A mutant (Figures 5F and 6D). Altogether, these data strongly support the idea that c-di-GMP binds to both PgaC and PgaD, resulting in the tight interaction and activation of the PgaCD GT complex.

Discussion

To transit from a planktonic, single cell to a biofilm-associated community 'lifestyle' bacteria undergo a complex and highly regulated process that is globally coordinated by the ubiquitous bacterial second messenger c-di-GMP (Schirmer and Jenal, 2009; Hengge, 2009). One of the key cellular processes directly stimulated by c-di-GMP is the production and secretion of exopolysaccharides that serve as protective biofilm matrix. Recently, several c-di-GMP receptor proteins were identified that regulate EPS production (Amikam and Galperin, 2006; Merighi *et al*, 2007; Lee *et al*, 2007; Whitney *et al*, 2012). However, their mode of action has remained elusive. To address the molecular principles of c-di-GMP-induced EPS production we have chosen the *E. coli* Pga system primarily for reasons of its relatively simple architecture. The secretion of poly-GlcNAc by the Pga machinery was linked to c-di-GMP signaling earlier (Kirillina *et al*, 2004; Boehm *et al*, 2009; Tagliabue *et al*, 2010; Pérez-Mendoza *et al*, 2011). However, the molecular mechanisms involved remained unclear and, despite of obvious analogies to other EPS secretion systems, none of the canonical c-di-GMP receptor domains is part of the Pga system.

We showed previously that the Pga system is regulated by c-di-GMP on the post-transcriptional level (Boehm *et al*, 2009). In this study, we close the gap by demonstrating that c-di-GMP

allosterically regulates the PgaCD glycosyltransferase complex in the inner membrane. The PgaCD complex represents a novel type c-di-GMP receptor, in which both membrane-integral proteins contribute to ligand binding, thereby mediating robust interaction, PgaD stabilization and activation of the two partners. This is the first example of a c-di-GMP receptor that relies on protein-protein interaction. Several lines of evidence support these findings. Only a PgaCD complex, but not PgaC or PgaD alone, showed specific and competitive ligand binding. Moreover, UV-crosslinking of radiolabeled c-di-GMP consistently and specifically labeled both PgaC and PgaD. Because of the close proximity that is needed for covalent zero-length crosslink formation, this strongly implies that amino acid residues from both proteins participate in the formation of the ligand-binding pocket. The observation that PgaC was incorporating more radioactivity than PgaD could reflect the nature of the c-di-GMP binding pocket, since not all amino acid residues show the same propensity for covalent crosslinking to a nucleotide ligand upon UV light irradiation (Meisenheimer and Koch, 1997). These results strongly argue against the possibility that the c-di-GMP binding pocket is entirely contained within PgaC with PgaD triggering the binding-competent conformation of its partner. Concomitant binding of c-di-GMP to PgaC and PgaD is further supported by genetic evidence. We isolated *pgaD* alleles that uncoupled the PgaCD complex from c-di-GMP signaling in terms of c-di-GMP binding, allosteric GT activation and biofilm formation. These constitutive mutations cluster within a short, positively charged region proximal to the second membrane-spanning domain of PgaD that likely contributes to c-di-GMP binding. In contrast, none of the activating *pgaC* alleles showed a completely c-di-GMP-'blind' phenotype, emphasizing the important role of PgaD in c-di-GMP-mediated GT activation.

Both *in vivo* and *in vitro* data suggest that c-di-GMP is absolutely essential for PgaCD GT activity and poly-GlcNAc-dependent biofilm formation. Our data indicate that c-di-GMP binds to the PgaCD complex with high affinity (K_{act} = 62 nM). Interestingly, c-di-GMP increased the velocity (V_{max}) of the GT complex, but not the affinity for its substrate UDP-GlcNAc. This is similar to the findings with cellulose synthase (Aloni *et al*, 1983; Ross *et al*, 1987) and implies that UDP-activated sugar molecules are not limiting under conditions that favor EPS synthesis and secretion. This, in turn, is in good agreement with the fact that the K_m of PgaCD (270 μM) lies well within the range of reported cellular UDP-GlcNAc concentrations in *E. coli* (Mengin-Lecreulx *et al*, 1989; Namboori and Graham, 2008). The strong effect of c-di-GMP on PgaCD activity raises the question of how the second messenger stimulates this enzyme complex. PgaC is a member of the processive GT-2 β-glycosyltransferase family, which are thought to function as monomers making use of two active site-containing domains, A and B, for the sugar polymerization reaction (Saxena

and Brown, 1997; Tlapak-Simmons *et al*, 1998; Ciocchini *et al*, 2006). But how would a growing polysaccharide chain be efficiently transferred across the hydrophobic membrane lipid barrier with as little as four transmembrane domains (TMDs) (Bobrov *et al*, 2008)? For the *Streptococcus* hyaluronan synthase, a structural homologue of PgaC, the interaction with cardiolipin molecules was suggested as a solution to this 'transfer dilemma' (Tlapak-Simmons *et al*, 1999). Based on our findings of c-di-GMP-mediated PgaCD complex activation, we propose a central role for PgaD in converting the PgaC GT into a secretion-competent conformation. In our model c-di-GMP binding to both PgaC and PgaD induces a conformational change that causes the integration of the two transmembrane helices of PgaD into the core of transmembrane domains formed by PgaC. This would convert the loosely associated GT complex into a stable, active and secretion-competent heterodimeric complex by opening up a pore for poly-GlcNAc translocation across the cytoplasmic membrane (Figures 8A and 8B). The presence of the two membrane-associated domains (MADs) 3 and 6 in the PgaC architecture of our model is based on the membrane topology model determined for the *Streptococcus* hyaluronan synthase, a homologous protein (Heldermon *et al*, 2001). In line with this, bioinformatic predictions indicate an increased probability for membrane association of regions 3 and 6 of PgaC. It is thus possible that the c-di-GMP-stimulated interaction between PgaC and PgaD recruits MADs 3 and 6 of PgaC into a secretion-competent transmembrane pore (Figure 8B). The regions in PgaC (R222) and PgaD (NKLR) proposed to be involved in the formation of the c-di-GMP binding site are well positioned to bring together PgaC MAD3 and PgaD TMD2 (Figures 8A and 8B). Such an arrangement would also explain the strong constitutive effect of the PgaC mutant V227L, as this mutation is located at the N-terminal face of MAD3, in the immediate vicinity of the proposed c-di-GMP binding site (Figure 8A). The formation of a membrane-integral heterodimeric complex as a functional secretion unit is the simplest model to concur with our findings that a PgaCD fusion protein is fully functional, that both proteins are absolutely required for poly-GlcNAc synthesis *in vivo* and *in vitro* and that the two transmembrane domains are the critical functional determinants of PgaD. Moreover, the observation that PgaD is strictly required for poly-GlcNAc secretion is in line with a structural requirement for this protein. The association of the GT with a second inner membrane protein essential for its activity seems to be a general phenomenon of homopolymeric EPS secretion systems (Keiski *et al*, 2010).

Among the organisms harboring a Pga-like poly-GlcNAc secretion system two subfamilies of PgaD proteins exist. All gram-negative bacteria that are devoid of c-di-GMP signaling harbor a *Staphylococcus epidermidis* IcaD-like (Gerke *et al*, 1998) homologue, while the presence of GGDEF

domains strongly correlates with PgaD-like proteins (and the presence of R222 in PgaC). This is striking since evidence is accumulating that *Staphylococcus* spp. are unable to synthesize c-di-GMP (Holland *et al*, 2008). It can thus be speculated that PgaD-like partners of the PgaC GT family interlink the activity of this EPS system with the cell's c-di-GMP circuitry. The observation that a PgaCD fusion protein is fully functional and responsive to c-di-GMP raised the question why nature has split this functional unit into two individual polypeptides. We would like to propose that the answer to this question is linked to the observed instability of PgaD when cellular levels of c-di-GMP are low. Rapid removal of PgaD under these conditions would irreversibly shut-off the Pga machinery and temporarily uncouple poly-GlcNAc synthesis and secretion from cellular c-di-GMP levels (Figure 8C). Reinstating poly-GlcNAc production in cells that went through a trough of c-di-GMP would require a derepressed Csr pathway allowing the resynthesis of all Pga components. Such a mechanism would thus elegantly equip the global Csr pathway (Timmermans and Van Melderen, 2010; Romeo *et al*, 2012) with a clear dominance over short-term fluctuations of c-di-GMP resulting from signal input into different DGCs and PDEs, and by that providing the basis for signaling specificity of c-di-GMP-controlled systems (Figure 8C).

In conclusion, this work shows that in *E. coli*, poly-GlcNAc-dependent biofilm formation is allosterically controlled through c-di-GMP binding to the membrane-anchored PgaCD complex. Since two proteins have to interact in order to form a ligand-binding pocket, the PgaCD complex represents a novel type c-di-GMP receptor. The elucidation of the details of the specific interaction between the allosteric ligand and the PgaCD complex will require careful biochemical and structural analysis.

Materials and methods

More detailed descriptions of Materials and methods are provided in the Supplementary data.

Membrane preparation

Overnight pre-cultures of strains AB1638 or AB2043 harboring the desired plasmid for protein overexpression (or strains AB1775, AB1776 and AB1777) were diluted 1:100 into 1 L LB medium and cultures were grown at 30°C to OD_{600} of 0.2, before expression of plasmid-borne genes was induced with 0.2% L-arabinose for 5 h. Cells were harvested by centrifugation, resuspended in 5-10 ml ice-cold French Press Buffer (50 mM HEPES pH 7, 5 mM $CaCl_2$, 1 mM DTT, Complete Mini EDTA-free protease inhibitors (Roche)) and lysed by passage three times through a French pressure cell (Vanderheiden *et al*, 1970). Lysate was clarified by centrifugation (27'000 g, 70 min,

4°C), before membranes were pelleted by ultracentrifugation (120'000 g, 90 min, 4°C). Membranes were generally resuspended in ~250 µl French Press Buffer and stored at -80°C.

Glycosyltransferase (GT) activity assays

Modified enzyme-coupled spectrophotometric assay. PgaCD GT activity was indirectly determined with a modified enzyme-coupled spectrophotometric assay (Baykov *et al*, 1988). Briefly, 50 µl reaction mixtures containing membranes from strains AB1775, AB1776 or AB1777 (approximately 10 mg/ml total protein) in GT Activity Buffer (50 mM HEPES pH 7, 5 mM $CaCl_2$, 5 mM $MgCl_2$) were incubated for 5 h at 30°C with or without 2 mM UDP-GlcNAc. The pH of the reactions was increased to 8-8.5 by adding 0.1 M NaOH and taking them up in SAP Buffer (50 mM Tris HCl pH 9, 10 mM $MgCl_2$), before reactions were incubated with 1.5 µl shrimp alkaline phosphatase (SAP) (Promega) for 80 min at 37°C. Phosphate content (indirect measure for UDP) was determined spectrophotometrically at 630 nm using the color reagent containing molybdate and malachite green (Baykov *et al*, 1988). Background value was subtracted.

FPLC anion exchange column assay. Standard 100 µl reaction mixtures contained membranes from strain AB2043 harboring the desired plasmid for protein overexpression (approximately 0.3-0.6 mg/ml total protein), varying UDP-GlcNAc concentrations (between 50 µM and 2 mM) and different c-di-GMP concentrations (between 0 µM and 2 µM) in GT Activity Buffer (50 mM HEPES pH 7, 5 mM $CaCl_2$, 5 mM $MgCl_2$). Whenever different mutants were compared, membrane inputs were adjusted with an immunoblot beforehand. Reactions were incubated between 0 min and 180 min at 30°C, before they were stopped by boiling for 5 min at 98°C. Samples were cleared by centrifugation (16'100 g, 1 min, 25°C) and supernatants were taken up in 900 µl 1 mM sodium acetate. Nucleotides UDP and UDP-GlcNAc were separated on an anion exchange column (1 ml Resource Q, GE Healthcare) mounted on an ÄKTA Purifier FPLC unit (GE Healthcare) with a linear gradient of sodium acetate from 1 mM to 1 M and monitored with Unicorn software. Initial linear PgaCD GT reaction velocities were determined by plotting integrated peak areas against reaction incubation times using GraphPad Prism.

C-di-GMP capture compound (cdG-CC) binding assay

CdG-CC (Caprotec Bioanalytics, Germany) experiments were carried out in 200 µl 12-tube PCR strips (Thermo Scientific) as previously described (Nesper *et al*, 2012) with some modifications. 100 µl samples generally contained membranes from strain AB1638 harboring the desired plasmid (approximately 3-4 mg/ml total protein) and 20 mM UDP-GlcNAc in Binding Buffer (20 mM HEPES pH 7.5, 50 mM potassium acetate, 10 mM magnesium acetate, 10% glycerol, 5 mM

$MgCl_2$, 1.5 mM $CaCl_2$). Whenever different mutants were compared, experiments were performed in the context of the PgaCD fusion protein and membrane inputs were adjusted with an immunoblot beforehand. A 12.5- or 125-fold molar excess of c-di-GMP or GTP was added to competition experiments and strips were preincubated for 30 min at 30°C with end-over-end agitation. After the addition of 0.8 μM or 8 μM cdG-CC, strips were wrapped in aluminum foil and incubated for 2 h at 30°C with end-over-end agitation. Samples were UV-irradiated at 310 nm for 4 min at 4°C using a caproBox (Caprotec Bioanalytics, Germany), before they were taken up in a final volume of 200 μl Capture Solubilization Buffer (50 mM Tris HCl pH 7.5, 1 mM EDTA, 1 M NaCl, 0.5% DDM) and solubilized for 4 h at 4°C with end-over-end agitation. After ultracentrifugation (100'000 g, 1 h, 4°C), an aliquot of the supernatants was saved and the rest incubated with 35 μl magnetic streptavidin beads (Dynabeads MyOne Streptavidin C1, Invitrogen) in PCR strips (Thermo Scientific) for 40 min at 4°C with end-over-end agitation. Beads were collected with a magnet (caproMag, Caprotec Bioanalytics, Germany) and washed 9x with 200 μl Capture Wash Buffer (50 mM Tris HCl pH 7.5, 1 mM EDTA, 1 M NaCl, 0.1% DDM), before captured proteins were analyzed by immunoblots. If different mutants were compared, band intensities were quantified using the ImageJ software and band intensities were normalized to the total solubilized protein amount of each sample.

UV-crosslinking with [$^{32/33}$P]c-di-GMP

UV light-induced crosslinking experiments were performed as previously described (Christen *et al*, 2005, 2006) in conical 96-well plates (Greiner Bio-One). 25 μl samples generally contained membranes from strain AB1638 harboring p2-3xF or p6a (approximately 30 mg/ml total protein) and 20 mM UDP-GlcNAc in Binding Buffer (20 mM HEPES pH 7.5, 50 mM potassium acetate, 10 mM magnesium acetate, 10% glycerol, 5 mM $MgCl_2$, 1.5 mM $CaCl_2$). Whenever different mutants were compared, membrane inputs were adjusted with an immunoblot beforehand. For competition experiments, a 100-fold molar excess of c-di-GMP or GTP was added. Plates were preincubated sealed with a foil for 35 min at 30°C on a rocking platform, before the addition of 1 μM or 2 μM radiolabeled [$^{32/33}$P]c-di-GMP. After a second incubation for 2 h at 30°C, foils were removed and 96-well plates were UV-irradiated at 254 nm for 20 min using a Bio-Link crosslinker (Vilber Lourmat, France). Thereafter, samples were taken up in a final volume of 200 μl Crosslinking Solubilization Buffer (50 mM Tris HCl pH 7.5, 200 mM NaCl, 5% glycerol, 1 mM DTT, 0.5% DDM) and solubilized overnight at 4°C with end-over-end agitation. After ultracentrifugation (100'000 g, 1 h, 4°C), supernatants were incubated with 40 μl anti-Flag M2 magnetic beads (Sigma) overnight at 4°C with end-over-end agitation. Beads were washed multiple times with IP

Wash Buffer B (50 mM Tris HCl pH 7.5, 1 M NaCl, 5% glycerol, 0.1% DDM) and the help of a magnet, before immunoprecipitated proteins were analyzed by Coomassie staining and autoradiography. If needed, band intensities were quantified using the ImageJ software and autoradiography band intensities were normalized to protein amounts on Coomassie-stained gels.

Supplementary data

Supplementary data are available at *The EMBO Journal* Online (http://www.embojournal.org).

Acknowledgements

We thank Jacob G. Malone for assistance with error-prone PCR, Alain Casanova for the construction of strain AB1313 and plasmid pAC551, Knut Ohlsen and Wilma Ziebuhr for the generous gift of antiserum against poly-GlcNAc and Régis Hallez for helpful advice and discussions. C-di-GMP measurements were provided by Prof. Volkhard Kaever from the Medizinische Hochschule Hannover. This work was supported by Swiss National Science Foundation grant 31003A_130469 to UJ and a fellowship from the Werner Siemens Foundation (Zug) to SS.

Author Contributions

SS, CL, AB and UJ conceived and designed the experiments. SS and CL performed the experiments. SS, CL, AB and UJ analyzed the data. SS and UJ wrote the paper.

Conflict of Interest

The authors declare that they have no conflict of interest.

References

Aloni Y, Cohen R, Benziman M, Delmer D (1983) Solubilization of the UDP-glucose:1,4-beta-D-Glucan 4-beta-D-Glucosyltransferase (Cellulose Synthase) from Acetobacter xylinum. *J Biol Chem* **258:** 4419–4423

Amikam D, Galperin MY (2006) PilZ domain is part of the bacterial c-di-GMP binding protein. *Bioinformatics* **22:** 3–6

Baykov AA, Evtushenko OA, Avaeva SM (1988) A malachite green procedure for orthophosphate determination and its use in alkaline phosphatase-based enzyme immunoassay. *Anal Biochem* **171:** 266–270

Becker S, Soares C, Porto LM (2009) Computational analysis suggests that virulence of Chromobacterium violaceum might be linked to biofilm formation and poly-NAG biosynthesis. *Genet Mol Biol* **32:** 640–644

Benach J, Swaminathan SS, Tamayo R, Handelman SK, Folta-Stogniew E, Ramos JE, Forouhar F, Neely H, Seetharaman J, Camilli A, Hunt JF (2007) The structural basis of cyclic diguanylate signal transduction by PilZ domains. *EMBO J* **26:** 5153–5166

Bentancor LV, O'Malley JM, Bozkurt-Guzel C, Pier GB, Maira-Litrán T (2012) Poly-N-acetyl-beta-(1-6)-glucosamine is a target for protective immunity against Acinetobacter baumannii infections. *Infect Immun* **80:** 651–656

Bobrov AG, Kirillina O, Forman S, Mack D, Perry RD (2008) Insights into Yersinia pestis biofilm development: topology and co-interaction of Hms inner membrane proteins involved in exopolysaccharide production. *Environ Microbiol* **10:** 1419–1432

Boehm A, Kaiser M, Li H, Spangler C, Kasper CA, Ackermann M, Kaever V, Sourjik V, Roth V, Jenal U (2010) Second messenger-mediated adjustment of bacterial swimming velocity. *Cell* **141:** 107–116

Boehm A, Steiner S, Zaehringer F, Casanova A, Hamburger F, Ritz D, Keck W, Ackermann M, Schirmer T, Jenal U (2009) Second messenger signalling governs Escherichia coli biofilm induction upon ribosomal stress. *Mol Microbiol* **72:** 1500–1516

Branda SS, Vik A, Friedman L, Kolter R (2005) Biofilms: the matrix revisited. *Trends Microbiol* **13:** 20–26

Cerca N, Maira-Litrán T, Jefferson KK, Grout M, Goldmann DA, Pier GB (2007) Protection against Escherichia coli infection by antibody to the Staphylococcus aureus poly-N-acetylglucosamine surface polysaccharide. *Proc Natl Acad Sci USA* **104:** 7528–7533

Choi AHK, Slamti L, Avci FY, Pier GB, Maira-Litrán T (2009) The pgaABCD locus of Acinetobacter baumannii encodes the production of poly-beta-1-6-N-acetylglucosamine, which is critical for biofilm formation. *J Bacteriol* **191:** 5953–5963

Christen B, Christen M, Paul R, Schmid F, Folcher M, Jenoe P, Meuwly M, Jenal U (2006) Allosteric control of cyclic di-GMP signaling. *J Biol Chem* **281:** 32015–32024

Christen M, Christen B, Folcher M, Schauerte A, Jenal U (2005) Identification and characterization of a cyclic di-GMP-specific phosphodiesterase and its allosteric control by GTP. *J Biol Chem* **280:** 30829–30837

Ciocchini AE, Roset MS, Briones G, Iñón de Iannino N, Ugalde RA (2006) Identification of active site residues of the inverting glycosyltransferase Cgs required for the synthesis of cyclic beta-1,2-glucan, a Brucella abortus virulence factor. *Glycobiology* **16:** 679–691

Conover MS, Sloan GP, Love CF, Sukumar N, Deora R (2010) The Bps polysaccharide of Bordetella pertussis promotes colonization and biofilm formation in the nose by functioning as an adhesin. *Mol Microbiol* **77:** 1439–1455

Costerton JW, Stewart PS, Greenberg EP (1999) Bacterial biofilms: a common cause of persistent infections. *Science* **284:** 1318–1322

Davies D (2003) Understanding biofilm resistance to antibacterial agents. *Nat Rev Drug Discov* **2:** 114–122

Fang X, Gomelsky M (2010) A post-translational, c-di-GMP-dependent mechanism regulating flagellar motility. *Mol Microbiol* **76:** 1295–1305

Flemming H-C, Wingender J (2010) The biofilm matrix. *Nat Rev Microbiol* **8:** 623–633

Forman S, Bobrov AG, Kirillina O, Craig SK, Abney J, Fetherston JD, Perry RD (2006) Identification of critical amino acid residues in the plague biofilm Hms proteins. *Microbiology* **152:** 3399–3410

Fux CA, Costerton JW, Stewart PS, Stoodley P (2005) Survival strategies of infectious biofilms. *Trends Microbiol* **13:** 34–40

Gerke C, Kraft A, Süssmuth R, Schweitzer O, Götz F (1998) Characterization of the N-acetylglucosaminyltransferase activity involved in the biosynthesis of the Staphylococcus epidermidis polysaccharide intercellular adhesin. *J Biol Chem* **273:** 18586–18593

Habazettl J, Allan MG, Jenal U, Grzesiek S (2011) Solution structure of the PilZ domain protein PA4608 complex with cyclic di-GMP identifies charge clustering as molecular readout. *J Biol Chem* **286:** 14304–14314

Hall-Stoodley L, Costerton JW, Stoodley P (2004) Bacterial biofilms: from the natural environment to infectious diseases. *Nat Rev Microbiol* **2:** 95–108

Heldermon C, DeAngelis PL, Weigel PH (2001) Topological organization of the hyaluronan synthase from Streptococcus pyogenes. *J Biol Chem* **276:** 2037–2046

Hengge R (2009) Principles of c-di-GMP signalling in bacteria. *Nat Rev Microbiol* **7:** 263–273

Holland LM, O'Donnell ST, Ryjenkov DA, Gomelsky L, Slater SR, Fey PD, Gomelsky M, O'Gara JP (2008) A staphylococcal GGDEF domain protein regulates biofilm formation independently of cyclic dimeric GMP. *J Bacteriol* **190:** 5178–5189

Itoh Y, Rice JD, Goller C, Pannuri A, Taylor J, Meisner J, Beveridge TJ, Preston JF, Romeo T (2008) Roles of pgaABCD genes in synthesis, modification, and export of the Escherichia coli biofilm adhesin poly-beta-1,6-N-acetyl-D-glucosamine. *J Bacteriol* **190:** 3670–3680

Izano EA, Sadovskaya I, Vinogradov E, Mulks MH, Velliyagounder K, Ragunath C, Kher WB, Ramasubbu N, Jabbouri S, Perry MB, Kaplan JB (2007) Poly-N-acetylglucosamine mediates biofilm formation and antibiotic resistance in Actinobacillus pleuropneumoniae. *Microb Pathog* **43:** 1–9

Izano EA, Sadovskaya I, Wang H, Vinogradov E, Ragunath C, Ramasubbu N, Jabbouri S, Perry MB, Kaplan JB (2008) Poly-N-acetylglucosamine mediates biofilm formation and detergent resistance in Aggregatibacter actinomycetemcomitans. *Microb Pathog* **44:** 52–60

Jonas K, Edwards AN, Simm R, Romeo T, Römling U, Melefors O (2008) The RNA binding protein CsrA controls cyclic di-GMP metabolism by directly regulating the expression of GGDEF proteins. *Mol Microbiol* **70:** 236–257

Karimova G, Pidoux J, Ullmann A, Ladant D (1998) A bacterial two-hybrid system based on a reconstituted signal transduction pathway. *Proc Natl Acad Sci USA* **95:** 5752–5756

Keiski C-L, Harwich M, Jain S, Neculai AM, Yip P, Robinson H, Whitney JC, Riley L, Burrows LL, Ohman DE, Howell PL (2010) AlgK is a TPR-containing protein and the periplasmic component of a novel exopolysaccharide secretin. *Structure* **18:** 265–273

Kirillina O, Fetherston JD, Bobrov AG, Abney J, Perry RD (2004) HmsP, a putative phosphodiesterase, and HmsT, a putative diguanylate cyclase, control Hms-dependent biofilm formation in Yersinia pestis. *Mol Microbiol* **54:** 75–88

Lee VT, Matewish JM, Kessler JL, Hyodo M, Hayakawa Y, Lory S (2007) A cyclic-di-GMP receptor required for bacterial exopolysaccharide production. *Mol Microbiol* **65:** 1474–1484

Mah TF, O'Toole GA (2001) Mechanisms of biofilm resistance to antimicrobial agents. *Trends Microbiol* **9:** 34–39

Maira-Litrán T, Kropec A, Goldmann DA, Pier GB (2005) Comparative opsonic and protective activities of Staphylococcus aureus conjugate vaccines containing native or deacetylated Staphylococcal poly-N-acetyl-beta-(1-6)-glucosamine. *Infect Immun* **73:** 6752–6762

Meisenheimer KM, Koch TH (1997) Photocross-linking of nucleic acids to associated proteins. *Crit Rev Biochem Mol* **32:** 101–140

Mengin-Lecreulx D, Siegel E, van Heijenoort J (1989) Variations in UDP-N-acetylglucosamine and UDP-N-acetylmuramyl-pentapeptide pools in Escherichia coli after inhibition of protein synthesis. *J Bacteriol* **171:** 3282–3287

Merighi M, Lee VT, Hyodo M, Hayakawa Y, Lory S (2007) The second messenger bis-(3'-5')-cyclic-GMP and its PilZ domain-containing receptor Alg44 are required for alginate biosynthesis in Pseudomonas aeruginosa. *Mol Microbiol* **65:** 876–895

Monteiro C, Saxena I, Wang X, Kader A, Bokranz W, Simm R, Nobles D, Chromek M, Brauner A, Brown RMJ, Römling U (2009) Characterization of cellulose production in Escherichia coli Nissle 1917 and its biological consequences. *Environ Microbiol* **11:** 1105–1116

Namboori SC, Graham DE (2008) Enzymatic analysis of uridine diphosphate N-acetyl-D-glucosamine. *Anal Biochem* **381:** 94–100

Nesper J, Reinders A, Glatter T, Schmidt A, Jenal U (2012) A novel capture compound for the identification and analysis of cyclic di-GMP binding proteins. *J Prot* **75:** 4874–4878

O'Gara JP (2007) ica and beyond: biofilm mechanisms and regulation in Staphylococcus epidermidis and Staphylococcus aureus. *FEMS Microbiol Lett* **270:** 179–188

Paul K, Nieto V, Carlquist WC, Blair DF, Harshey RM (2010) The c-di-GMP binding protein YcgR controls flagellar motor direction and speed to affect chemotaxis by a "backstop brake" mechanism. *Mol Cell* **38:** 128–139

Paul R, Weiser S, Amiot NC, Chan C, Schirmer T, Giese B, Jenal U (2004) Cell cycle-dependent dynamic localization of a bacterial response regulator with a novel di-guanylate cyclase output domain. *Genes Dev* **18:** 715–727

Pesavento C, Becker G, Sommerfeldt N, Possling A, Tschowri N, Mehlis A, Hengge R (2008) Inverse regulatory coordination of motility and curli-mediated adhesion in Escherichia coli. *Genes Dev* **22:** 2434–2446

Povolotsky TL, Hengge R (2012) “Life-style” control networks in Escherichia coli: Signaling by the second messenger c-di-GMP. *J Biotechnol* **160:** 10–16

Pérez-Mendoza D, Coulthurst SJ, Sanjuán J, Salmond GPC (2011) N-acetyl-glucosamine-dependent biofilm formation in Pectobacterium atrosepticum is cryptic and activated by elevated c-di-GMP levels. *Microbiology* **157:** 3340–3348

Romeo T, Gong M, Liu MY, Brun-Zinkernagel A (1993) Identification and molecular characterization of csrA, a pleiotropic gene from Escherichia coli that affects glycogen biosynthesis, gluconeogenesis, cell size, and surface properties. *J Bacteriol* **175:** 4744–4755

Romeo T, Vakulskas CA, Babitzke P (2012) Post-transcriptional regulation on a global scale: form and function of Csr/Rsm systems. *Environ Microbiol*

Ross P, Weinhouse H, Aloni Y, Michaeli D, Weinberger-Ohana P, Mayer R, Braun S, Vroom E de, Van der Marel GA, Van Broom JH, Benziman M (1987) Regulation of cellulose synthesis in Acetobacter xylinum by cyclic diguanylic acid. *Nature* **325:** 279–281

Ryan RP, Fouhy Y, Lucey JF, Crossman LC, Spiro S, He Y-W, Zhang L-H, Heeb S, Cámara M, Williams P, Dow JM (2006) Cell-cell signaling in Xanthomonas campestris involves an HD-GYP domain protein that functions in cyclic di-GMP turnover. *Proc Natl Acad Sci USA* **103:** 6712–6717

Saxena IM, Brown RM (1997) Identification of cellulose synthase(s) in higher plants: sequence analysis of processive beta-glycosyltransferases with the common motif “D, D, D35Q(R,Q)XRW”. *Cellulose* **4:** 33–49

Saxena IM, Brown RM, Dandekar T (2001) Structure-function characterization of cellulose synthase: relationship to other glycosyltransferases. *Phytochemistry* **57:** 1135–1148

Schirmer T, Jenal U (2009) Structural and mechanistic determinants of c-di-GMP signalling. *Nat Rev Microbiol* **7:** 724–735

Skurnik D, Davis MRJ, Benedetti D, Moravec KL, Cywes-Bentley C, Roux D, Traficante DC, Walsh RL, Maria-Litràn T, Cassidy SK, Hermos CR, Martin TR, Thakkallapalli EL, Vargas SO, McAdam AJ, Lieberman TD, Kishony R, LiPuma JJ, Pier GB, Goldberg JB, *et al* (2012) Targeting pan-resistant bacteria with antibodies to a broadly conserved surface polysaccharide expressed during infection. *J Infect Dis* **205:** 1709–1718

Sondermann H, Shikuma NJ, Yildiz FH (2011) You’ve come a long way: c-di-GMP signaling. *Curr Opin Microbiol* **15:** 140–146

Sonnhammer EL, von Heijne G, Krogh A (1998) A hidden Markov model for predicting transmembrane helices in protein sequences. *Proceedings International Conference on Intelligent Systems for Molecular Biology* **6:** 175–182

Suzuki K, Babitzke P, Kushner SR, Romeo T (2006) Identification of a novel regulatory protein (CsrD) that targets the global regulatory RNAs CsrB and CsrC for degradation by RNase E. *Genes Dev* **20:** 2605–2617

Tagliabue L, Antoniani D, Maciag A, Bocci P, Raffaelli N, Landini P (2010) The diguanylate cyclase YddV controls production of the exopolysaccharide poly-N-acetylglucosamine (PNAG) through regulation of the PNAG biosynthetic pgaABCD operon. *Microbiology* **156:** 2901–2911

Timmermans J, Van Melderen L (2010) Post-transcriptional global regulation by CsrA in bacteria. *Cell Mol Life Sci* **67:** 2897–2908

Tlapak-Simmons VL, Baggenstoss BA, Clyne T, Weigel PH (1999) Purification and lipid dependence of the recombinant hyaluronan synthases from Streptococcus pyogenes and Streptococcus equisimilis. *J Biol Chem* **274:** 4239–4245

Tlapak-Simmons VL, Kempner ES, Baggenstoss BA, Weigel PH (1998) The active Streptococcal hyaluronan synthases (HASs) contain a single HAS monomer and multiple cardiolipin molecules. *J Biol Chem* **273:** 26100–26109

Tuckerman JR, Gonzalez G, Gilles-Gonzalez M-A (2011) Cyclic di-GMP activation of polynucleotide phosphorylase signal-dependent RNA processing. *J Mol Biol* **407:** 633–639

Vanderheiden GJ, Fairchild AC, Jago GR (1970) Construction of a laboratory press for use with the French pressure cell. *Appl Microbiol* **19:** 875–877

Wang X, Dubey AK, Suzuki K, Baker CS, Babitzke P, Romeo T (2005) CsrA post-transcriptionally represses pgaABCD, responsible for synthesis of a biofilm polysaccharide adhesin of Escherichia coli. *Mol Microbiol* **56:** 1648–1663

Wang X, Preston JF, Romeo T (2004) The pgaABCD locus of Escherichia coli promotes the synthesis of a polysaccharide adhesin required for biofilm formation. *J Bacteriol* **186:** 2724–2734

Weigel PH, DeAngelis PL (2007) Hyaluronan synthases: a decade-plus of novel glycosyltransferases. *J Biol Chem* **282:** 36777–36781

Whitney JC, Colvin KM, Marmont LS, Robinson H, Parsek MR, Howell PL (2012) Structure of the cytoplasmic region of PelD, a degenerate diguanylate cyclase receptor that regulates exopolysaccharide production in Pseudomonas aeruginosa. *J Biol Chem* **287:** 23582–23593

Yakandawala N, Gawande PV, LoVetri K, Cardona ST, Romeo T, Nitz M, Madhyastha S (2011) Characterization of the poly-beta-1,6-N-acetylglucosamine polysaccharide component of Burkholderia biofilms. *Appl Environ Microbiol* **77:** 8303–8309

Figure legends

Figure 1 C-di-GMP controls PgaD stability in a PgaC-dependent manner. (A) Schematic representation of the *E. coli* Pga machinery. See text for details. IM = inner membrane, PP = periplasm, OM = outer membrane. (B) Immunoblot analysis of 3xFlag-tagged Pga proteins in the *E. coli* control strain and Δ*ydeH* mutant. The native *pga* promoter (left panel) was replaced with the P_{ara} promoter (right panel). Expression of the *araB-pgaA* translational fusion was induced with 0.0002% L-arabinose. (C) PgaD levels depend on PgaC and c-di-GMP. Immunoblots of PgaD-3xFlag are shown for the indicated mutant strains. Expression of *pgaC* was induced with 0.0002% L-arabinose (left panel) and with 0%, 0.0002% and 0.2% L-arabinose (right panel). (D) Graph showing relative PgaD levels upon blocking protein biosynthesis in exponentially growing cells as an average of two independent experiments with standard deviations. Expression of the heterologous DGC *dgcA* and its active site mutant $dgcA^{mut}$ (D164N) was not induced (leaky expression). (E) Biofilm formation of strains carrying multiple deletions in genes predicted to encode DGCs. The Δ7 strain carries a total of seven deletions (Δ*ydeH*, Δ*ycdT*, Δ*yegE*, Δ*yfiN*, Δ*yhjK*, Δ*ydaM*, Δ*yneF*). Error bars are standard deviations. A representative dataset of the relative cellular c-di-GMP concentrations of the strains is indicated. n/a = not available, bld = below limit of detection. Inset: Immunoblot of PgaD-3xFlag in the control strain and the Δ7 mutant.

Figure 2 C-di-GMP enhances PgaC-PgaD interaction. (A) PgaC-6xHis and PgaD-3xFlag co-immunoprecipitate from detergent-solubilized membranes. Anti-Flag and protein A (mock) IPs were analyzed by immunoblots using antibodies against the specific tags. The protein fraction that failed to bind to the beads is indicated (sn = supernatant). 2 M urea was present during the IP procedure as indicated. (B) Co-immunoprecipitation of PgaC and PgaD-3xFlag from detergent-solubilized membranes of control strain and Δ7 mutant cells overexpressing *pgaC* and *pgaD*. IP samples were analyzed by Coomassie staining. HC and LC mark heavy and light chains of IgG. (C) Bacterial two-hybrid (BacTH) analysis of PgaC-PgaD interaction. Presence of T18 and T25 fusions is indicated. Zip indicates the leucine zipper positive control. (D) BacTH analysis of c-di-GMP-stimulated PgaC-PgaD interaction. Left panel: Interaction in the presence of a plasmid-borne copy of *dgcA* or its active site mutant $dgcA^{mut}$ (D164N). Alleles were induced with 0.2% L-arabinose. Right panel: Interaction in strains lacking the DGC YdeH or multiple DGCs (Δ7). See Supplementary Figure 2 for the quantification of interaction strengths. (E) A PgaCD fusion protein is fully functional. Biofilm formation and protein levels of 3xFlag-tagged PgaD or PgaCD fusion protein (PgaCDf) are indicated for the control strain (black bars) and a Δ*ydeH* mutant (grey bars). Error bars are standard deviations.

Figure 3 C-di-GMP allosterically stimulates PgaCD glycosyltransferase activity *in vitro*. (A) GT activity depends on an intact PgaCD complex. Enzyme activities were determined using control strain membranes containing PgaC, PgaD or both proteins in the presence (2 mM) or absence of the substrate UDP-GlcNAc. A representative dataset is shown. (B) Microscopic analysis of the viscous poly-GlcNAc reaction product. Membranes were incubated with 30 mM UDP-GlcNAc for 5 h at 30°C. Scale bars are indicated: 15 μm. (C) Determination of the PgaCD K_m for UDP-GlcNAc. Membranes of a Δ7 mutant containing PgaC and PgaD were incubated with increasing concentrations of UDP-GlcNAc in the presence of 1 μM c-di-GMP. Data represent an average of two independent experiments with standard deviations. (D) Stimulatory effect of c-di-GMP on PgaCD GT activity (K_{act}). Membranes of a Δ7 mutant containing PgaC and PgaD were incubated with increasing concentrations of c-di-GMP in the presence of 50 μM UDP-GlcNAc. A representative dataset is shown. (E) Lineweaver-Burk plot analysis of PgaCD GT activity. Membranes of a Δ7 mutant containing PgaC and PgaD were incubated with increasing concentrations of UDP-GlcNAc in the presence of a non-saturating (0.03 μM) and a saturating (1 μM) c-di-GMP concentration. Negative reciprocal K_m is indicated. A representative dataset is shown. GraphPad Prism was used for curve fitting and linear regression. a.u. = arbitrary unit.

Figure 4 Specific binding of c-di-GMP requires PgaC and PgaD. (A) Immunoblot of PgaD captured from membranes containing PgaC and PgaD-3xFlag. Presence of cdG-CC and competing nucleotides is indicated. (B) Immunoblots of PgaC, PgaD and PgaCD fusion protein (PgaCDf) captured from membranes containing PgaC and PgaD-3xFlag (1st panel), PgaCDf-3xFlag (2nd panel), PgaC-3xFlag (3rd panel), PgaD-3xFlag (4th panel) or PgaC-3xFlag and PgaD-3xFlag (5th panel). Presence of cdG-CC and competing nucleotides is indicated. SDS-resistant heterodimeric PgaCD complexes are indicated (PgaCD). (C) Specific labeling of PgaC and PgaD with [^{33}P]c-di-GMP. Membranes containing PgaC-3xFlag and PgaD-3xFlag were UV-crosslinked in the presence of [^{33}P]c-di-GMP and competing nucleotides as indicated. Coomassie staining (left panel) and autoradiography (right panel) are shown. HC and LC mark heavy and light chains of IgG. SDS-resistant heterodimeric PgaCD complexes are indicated (PgaCD). (D) Absence of PgaD abolishes c-di-GMP binding. Membranes containing PgaC-3xFlag and PgaD-3xFlag (left panels) or PgaC-3xFlag (right panel) were UV-crosslinked in the presence of [^{32}P]c-di-GMP and competing nucleotides as indicated. Only autoradiographies are shown.

Figure 5 Mutations in PgaD render the PgaCD complex constitutively active and independent of c-di-GMP. (A) Predicted topology of PgaD. Positions of c-di-GMP-independent (orange) and loss-of-function mutations (red) within the most conserved region of PgaD (grey) are indicated. Sites of C-terminal PgaD truncations are marked by triangles. IM = inner membrane, PP = periplasm. Transmembrane helices were predicted using the TMHMM server (Sonnhammer *et al*, 1998). (B) Biofilm formation of strains expressing C-terminally truncated *pgaD* alleles as a function of cellular c-di-GMP concentrations. The last residue of each mutant is indicated (see Figure 5A). Δ7 strains harboring individual *pgaD* alleles contained plasmids with an IPTG-inducible copy of the heterologous DGC *wspR* (p*wspR*) or control plasmids (vector). Expression of plasmid-borne *pgaD* alleles was induced with 0.2% (left graph) and 0.02% L-arabinose (right graph). Error bars are standard deviations. (C) Contribution of *pgaD* mutants to biofilm formation is shown in the control strain (black bars) and the Δ7 mutant (grey bars). Isolated constitutive alleles are underlined. Error bars are standard deviations. (D) Immunoblot analysis of steady state levels of wild-type and mutant forms of PgaD-3xFlag in the control strain and the Δ7 mutant. (E) C-di-GMP-dependent PgaCD GT activity. Membranes of a Δ7 mutant containing either PgaD wild-type or mutant forms were incubated with (black bars) or without c-di-GMP (grey bars) in the presence of 300 μM UDP-GlcNAc. PgaD mutant variants were expressed as PgaCD fusion proteins. A representative dataset is shown with standard errors. a.u. = arbitrary unit. (F) The PgaD mutant N75D,K76E is strongly impaired in c-di-GMP binding. Relative amounts of PgaD wild-type or mutant forms captured in the presence (black bars) or absence of excess c-di-GMP (grey bars) are shown as an average of two independent experiments with standard deviations. PgaD variants were expressed as PgaCD fusion proteins.

Figure 6 A constitutive PgaD mutant rescues a PgaC mutant unable to bind c-di-GMP. (A) Constitutive *pgaC* mutants show partial c-di-GMP independence. Contribution of *pgaC* mutants to biofilm formation is shown in the control strain (black bars) and the Δ7 mutant (grey bars). Isolated constitutive alleles are underlined. Error bars are standard deviations. (B) Immunoblot analysis of PgaD-3xFlag in the control strain and the Δ7 mutant expressing different *pgaC* alleles. (C) Mutational analysis of conserved arginine residues of PgaC (see text and Supplementary Figure 6D). Biofilm formation was determined for strains expressing the respective PgaC variants as PgaCD fusion proteins. R198D was included as a control as this arginine is also conserved in organisms that lack c-di-GMP. Error bars are standard deviations. (D) The PgaC R222A mutant is strongly impaired in c-di-GMP binding. A representative dataset of the relative amounts of PgaC wild-type or mutant forms captured in the presence (black bars) or absence of excess c-di-GMP

(grey bars) is shown. PgaC variants were expressed as PgaCD fusion proteins. (E) The constitutive PgaD N75D,K76E mutant rescues the PgaC R222A mutant deficient in c-di-GMP binding. Biofilm formation was determined for strains expressing different *pgaC* and/or *pgaD* alleles in the control strain (black bars) and the Δ7 mutant (grey bars). Error bars are standard deviations.

Figure 7 C-di-GMP directly binds to both PgaC and PgaD. Membranes containing wild-type and mutant forms of PgaC-3xFlag and/or PgaD-3xFlag were UV-crosslinked in the presence of [^{32}P]c-di-GMP and with (black bars) or without excess c-di-GMP (grey bars).
Quantification of PgaC (left graph) and PgaD (right graph) band intensities from (A) as an average of two independent experiments with standard deviations. Relative PgaC (upper graph) and PgaD (lower graph) autoradiography band intensities are shown as an average of two independent experiments with standard deviations.

Figure 8 Model for the allosteric activation of the PgaCD glycosyltransferase complex by c-di-GMP. (A) Topology models for PgaC and PgaD in the inner membrane. Orientations of PgaC transmembrane domains (TMDs) are based on this study, on TMHMM server predictions (Sonnhammer *et al*, 1998), on the proposed topology of the PgaC homologue from *Y. pestis* (Bobrov *et al*, 2008) and on a model proposed for the hyaluronan synthase from *Streptococcus pyogenes* (Heldermon *et al*, 2001; Weigel and DeAngelis, 2007). TMDs 1, 2, 4 and 5 are true transmembrane domains, while 3 and 6 are membrane-associated domains (MADs). Catalytic domains A and B with the active site of processive GT-2 β-glycosyltransferases are indicated (Saxena and Brown, 1997; Saxena *et al*, 2001). Regions proposed to be involved in c-di-GMP binding are highlighted in red. The position of the constitutive PgaC mutation V227L is indicated. CP = cytoplasm, IM = inner membrane, PP = periplasm. (B) C-di-GMP binding to the PgaCD complex stabilizes a heterodimeric complex to induce a secretion-competent conformation. Left: Top-view of the inactive transient state with loosely associated, highly unstable PgaD. Right: C-di-GMP binding induces a poly-GlcNAc secretion-competent state. (C) Model for the irreversible inactivation of PgaCD upon drop of cellular c-di-GMP levels. Signaling through the Csr cascade induces the synthesis of Pga components and the DGCs YdeH and YcdT. At low c-di-GMP concentrations (e.g. inactive DGCs or highly active PDEs) PgaD is rapidly removed by proteolysis, uncoupling the Pga machinery temporarily from c-di-GMP signaling. Only continuous or renewed input through the Csr signaling cascade will allow cells to reactivate poly-GlcNAc synthesis and secretion, thus providing the Csr cascade with signaling dominance over the enzymes directly regulating the cellular c-di-GMP level.

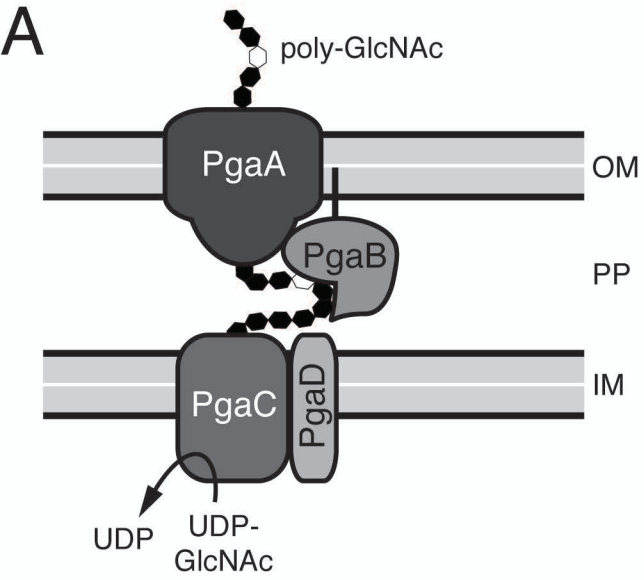
A
poly-GlcNAc
PgaA
OM
PgaB
PP
PgaC
PgaD
IM
UDP
UDP-
GlcNAc

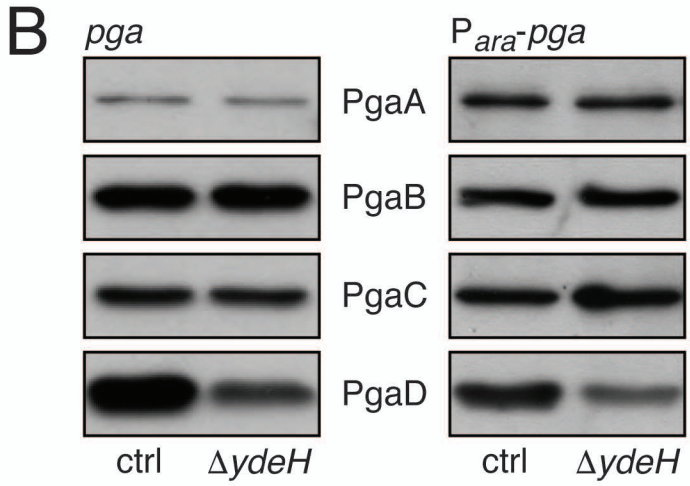
B
pga
P*ara*-*pga*
PgaA
PgaB
PgaC
PgaD
ctrl
Δ*ydeH*
ctrl
Δ*ydeH*

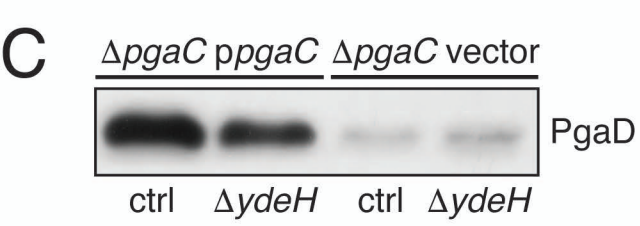
C
Δ*pgaC* p*pgaC*
Δ*pgaC* vector
PgaD
ctrl
Δ*ydeH*
ctrl
Δ*ydeH*

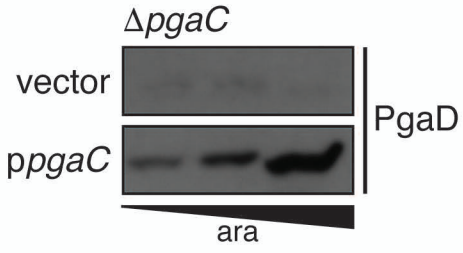
Δ*pgaC*
vector
p*pgaC*
PgaD
ara

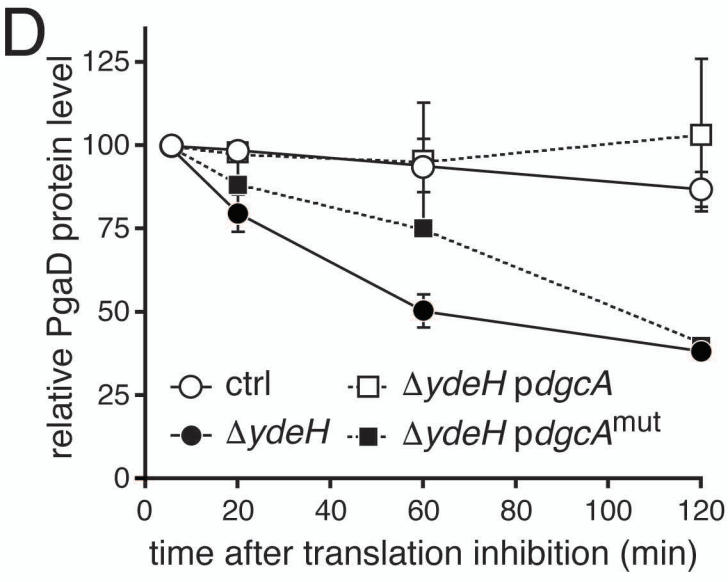
D
relative PgaD protein level
125
100
75
50
25
0
0
20
40
60
80
100
120
time after translation inhibition (min)
ctrl
Δ*ydeH*
Δ*ydeH* p*dgcA*
Δ*ydeH* p*dgcA*^{mut}

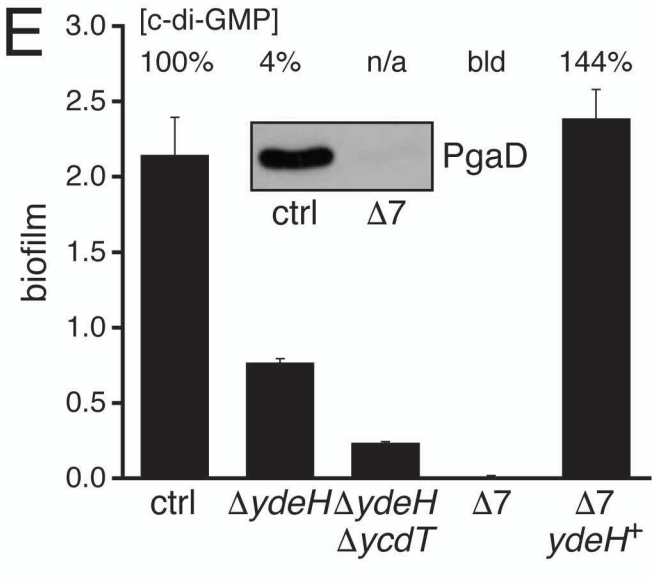
E
[c-di-GMP]
100%
4%
n/a
bld
144%
biofilm
3.0
2.5
2.0
1.5
1.0
0.5
0.0
PgaD
ctrl
Δ7
ctrl
Δ*ydeH*
Δ*ydeH* Δ*ycdT*
Δ7
Δ7 *ydeH*$^{+}$

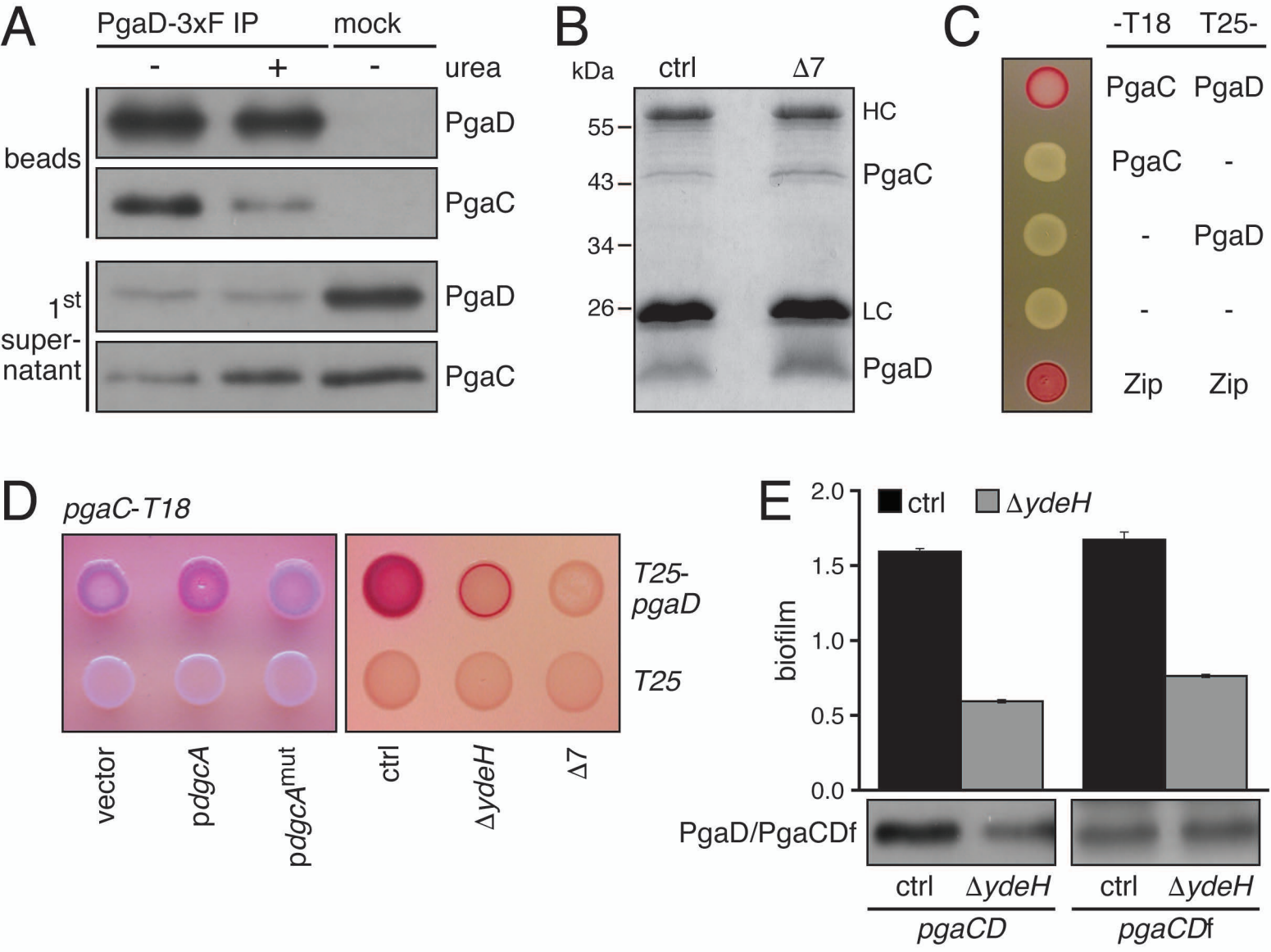
A
PgaD-3xF IP
mock
-
+
-
urea
beads
PgaD
PgaC
1st supernatant
PgaD
PgaC
B
kDa
ctrl
Δ7
55
43
34
26
HC
PgaC
LC
PgaD
C
-T18
T25-
PgaC
PgaD
PgaC
-
-
PgaD
-
-
Zip
Zip
D
pgaC-T18
T25-pgaD
T25
vector
pdgcA
pdgcAmut
ctrl
ΔydeH
Δ7
E
ctrl
ΔydeH
biofilm
2.0
1.5
1.0
0.5
0.0
PgaD/PgaCDf
ctrl
ΔydeH
ctrl
ΔydeH
pgaCD
pgaCDf

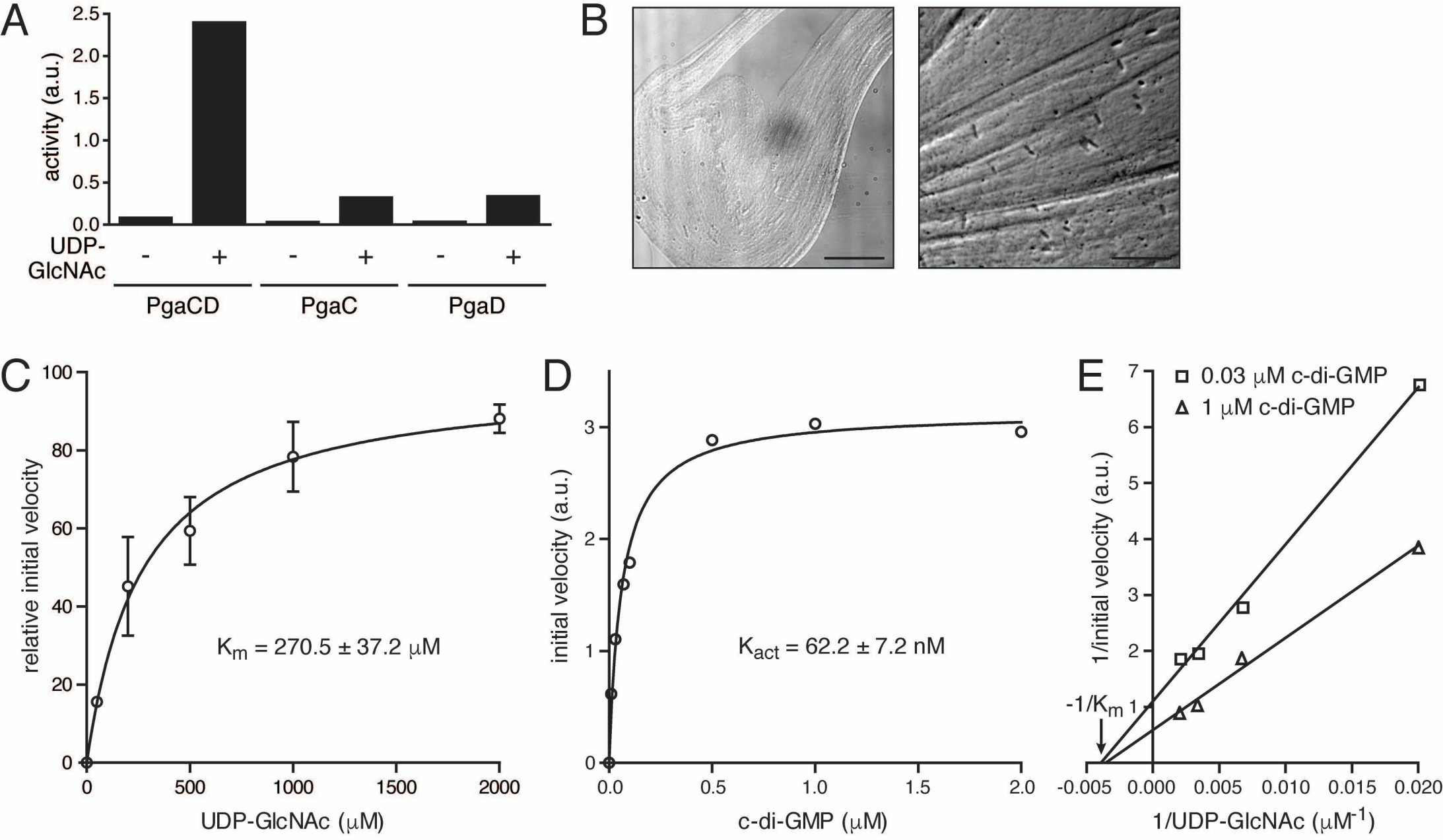
A
activity (a.u.)
2.5
2.0
1.5
1.0
0.5
0.0
UDP-GlcNAc
-
+
-
+
-
+
PgaCD
PgaC
PgaD
B
C
relative initial velocity
100
80
60
40
20
0
0
500
1000
1500
2000
UDP-GlcNAc (μM)
K_m = 270.5 ± 37.2 μM
D
initial velocity (a.u.)
3
2
1
0
0.0
0.5
1.0
1.5
2.0
c-di-GMP (μM)
K_{act} = 62.2 ± 7.2 nM
E
0.03 μM c-di-GMP
1 μM c-di-GMP
1/initial velocity (a.u.)
7
6
5
4
3
2
1
-1/K_m
-0.005
0.000
0.005
0.010
0.015
0.020
1/UDP-GlcNAc (μM^{-1})

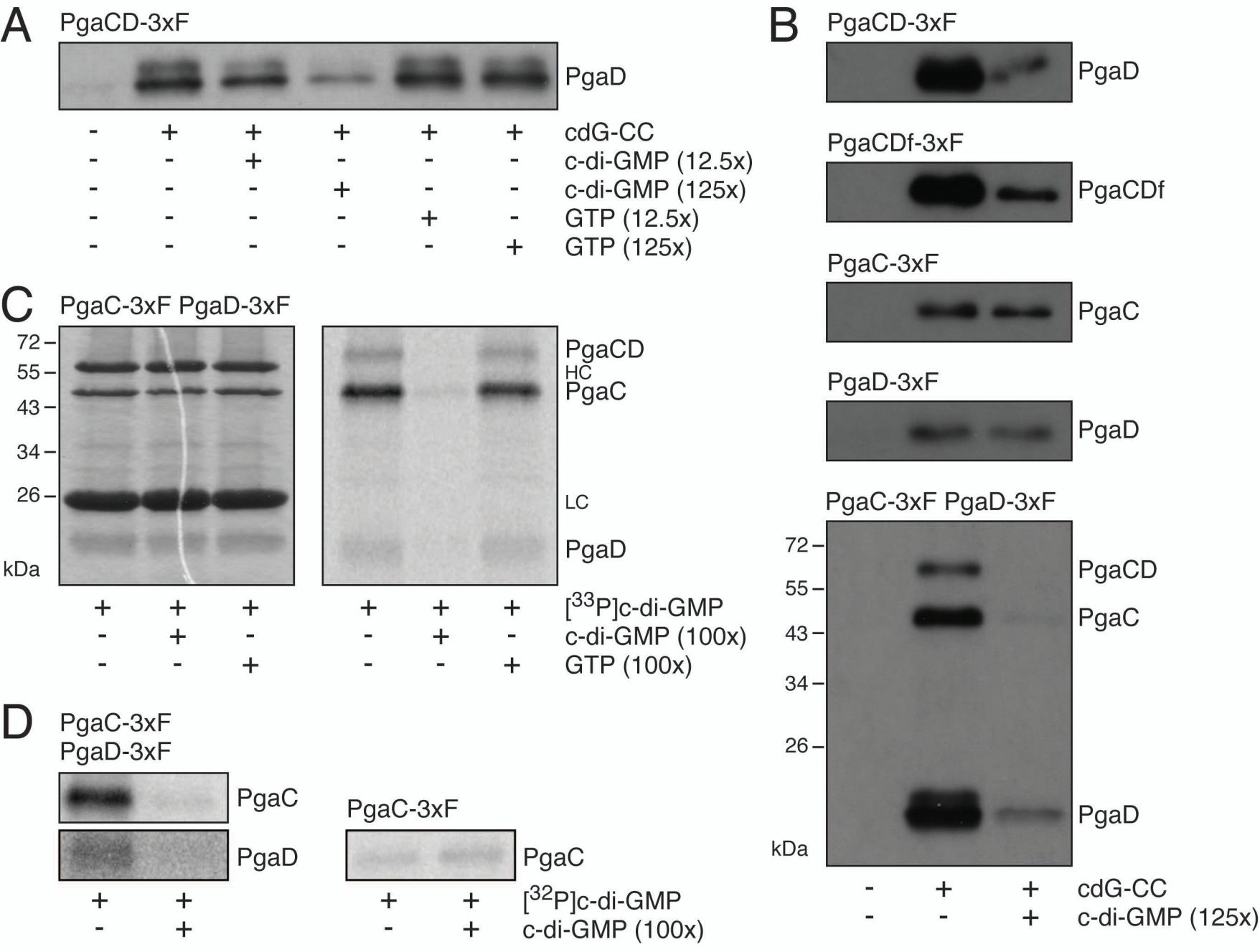
A
PgaCD-3xF
PgaD
- + + + + + cdG-CC
- - + - - - c-di-GMP (12.5x)
- - - + - - c-di-GMP (125x)
- - - - + - GTP (12.5x)
- - - - - + GTP (125x)
B
PgaCD-3xF
PgaD
PgaCDf-3xF
PgaCDf
PgaC-3xF
PgaC
PgaD-3xF
PgaD
PgaC-3xF PgaD-3xF
72
55
43
34
26
kDa
PgaCD
PgaC
- + + cdG-CC
- - + c-di-GMP (125x)
C
PgaC-3xF PgaD-3xF
72
55
43
34
26
kDa
PgaCD
HC
PgaC
LC
PgaD
+ + + + + + [33P]c-di-GMP
- + - - + - c-di-GMP (100x)
- - + - - + GTP (100x)
D
PgaC-3xF
PgaD-3xF
PgaC
PgaD
PgaC-3xF
PgaC
+ + + + [32P]c-di-GMP
- + - + c-di-GMP (100x)

Steiner *et al.* Figure 5

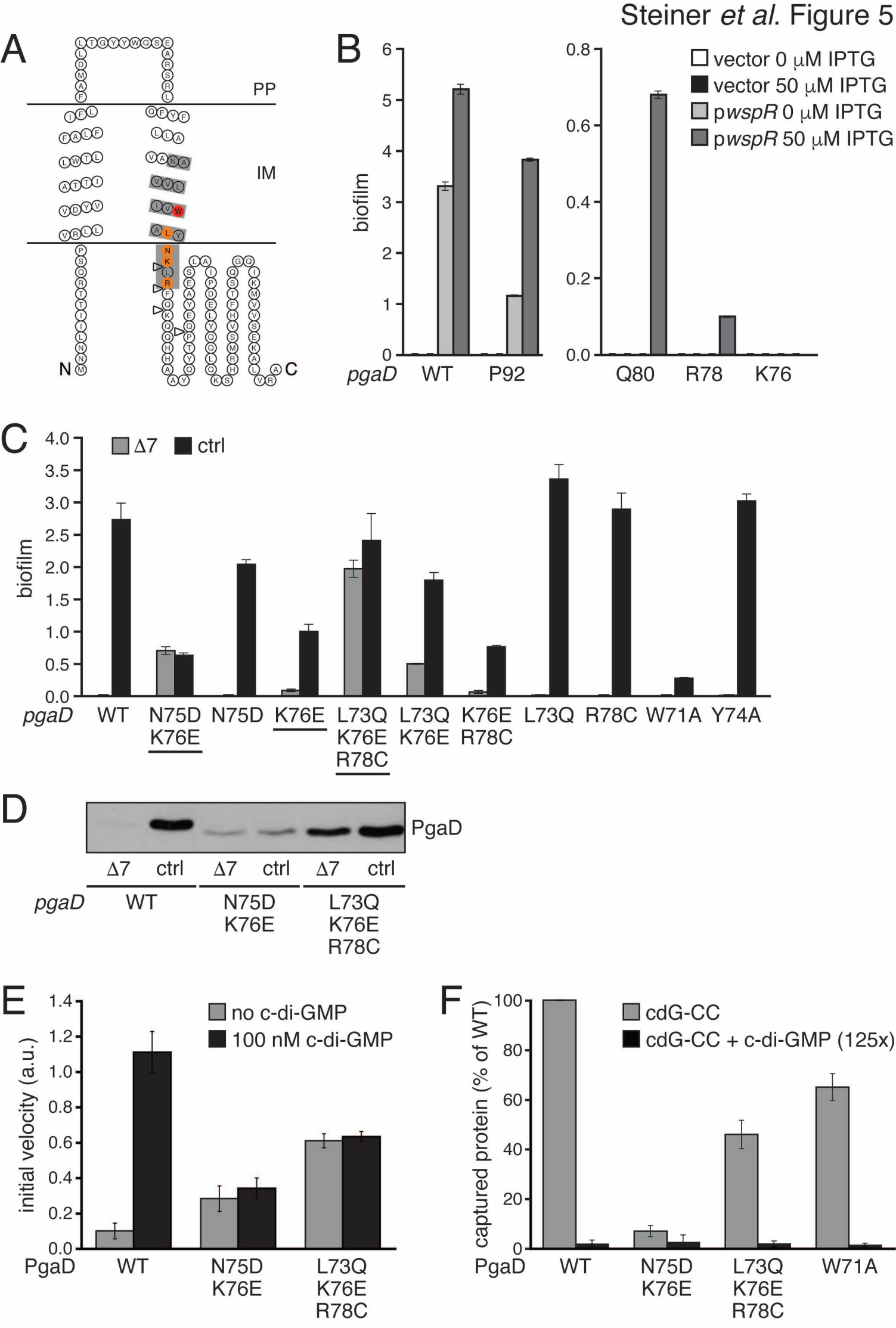

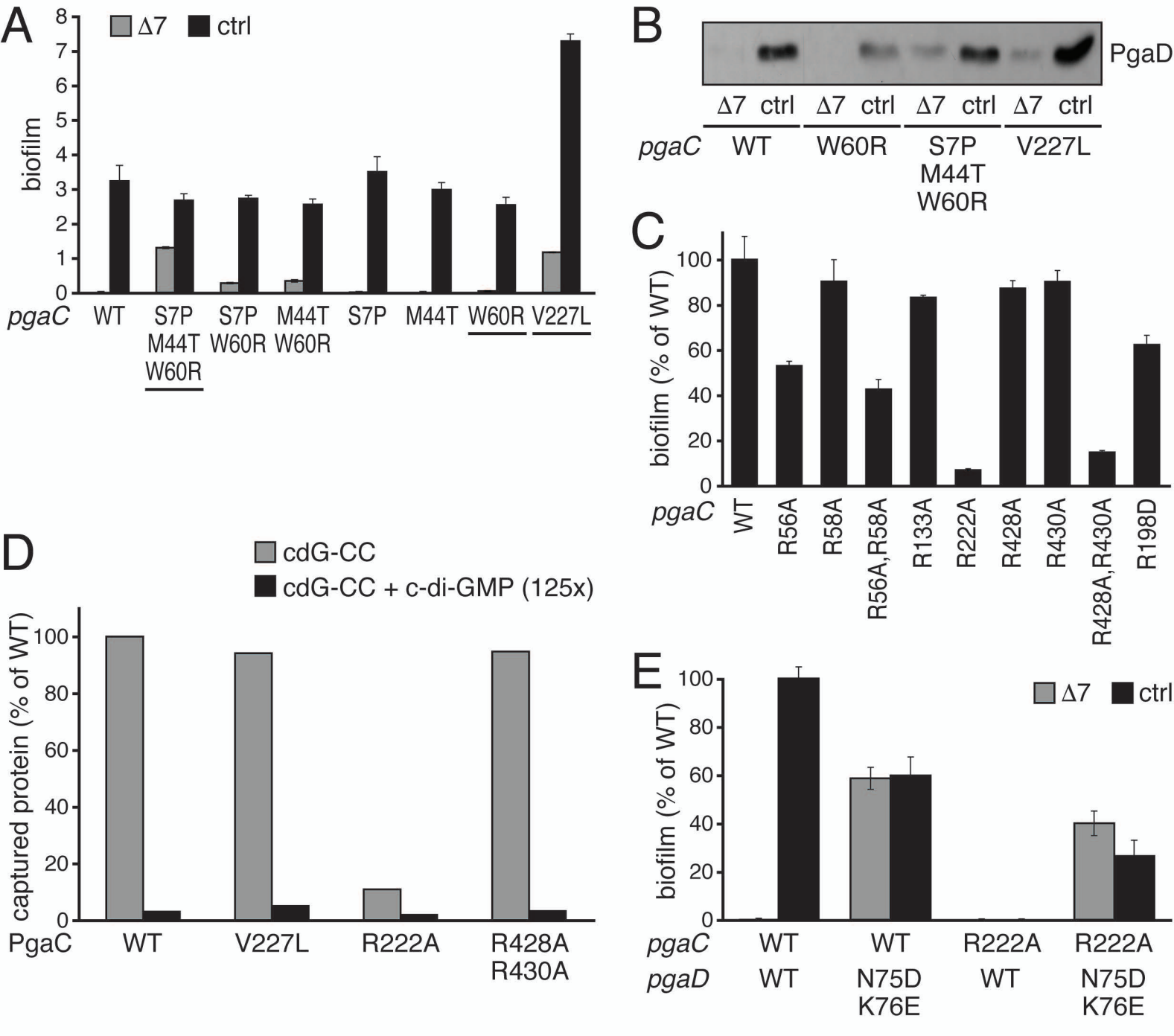
A
Δ7
ctrl
biofilm
pgaC
WT
S7P M44T W60R
S7P W60R
M44T W60R
S7P
M44T
W60R
V227L
B
PgaD
Δ7 ctrl Δ7 ctrl Δ7 ctrl Δ7 ctrl
pgaC
WT
W60R
S7P M44T W60R
V227L
C
biofilm (% of WT)
pgaC
WT
R56A
R58A
R56A,R58A
R133A
R222A
R428A
R430A
R428A,R430A
R198D
D
cdG-CC
cdG-CC + c-di-GMP (125x)
captured protein (% of WT)
PgaC
WT
V227L
R222A
R428A R430A
E
Δ7
ctrl
biofilm (% of WT)
pgaC
pgaD
WT WT
WT N75D K76E
R222A WT
R222A N75D K76E

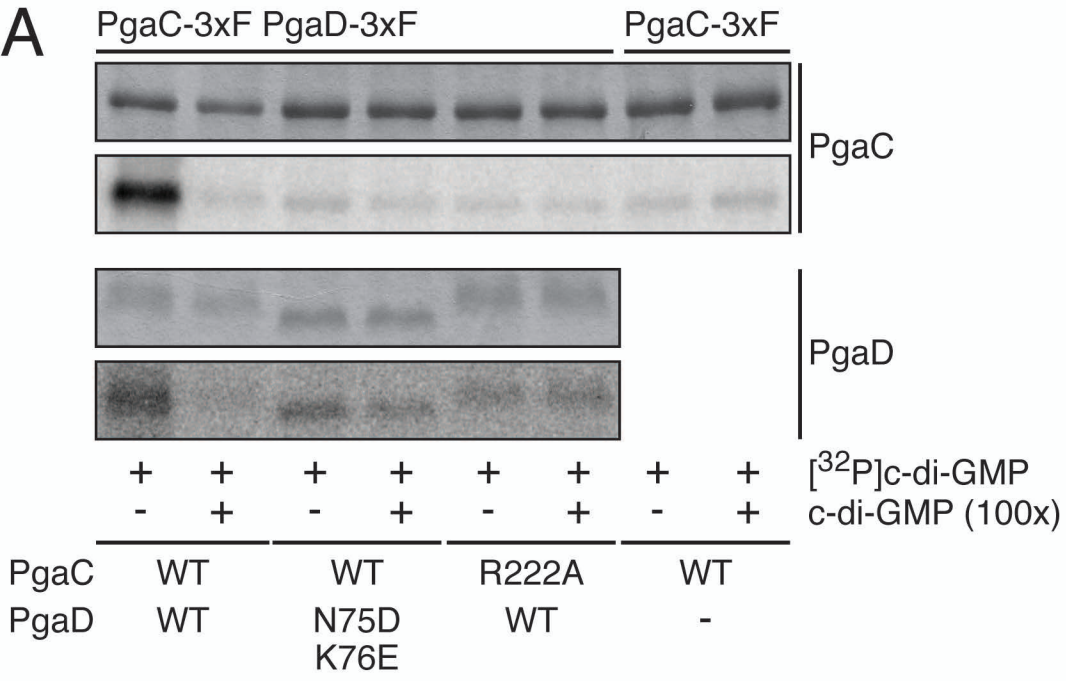
A
PgaC-3xF PgaD-3xF
PgaC-3xF
PgaC
PgaD
+ + + + + + + + [32P]c-di-GMP
- + - + - + - + c-di-GMP (100x)
PgaC WT WT R222A WT
PgaD WT N75D K76E WT -

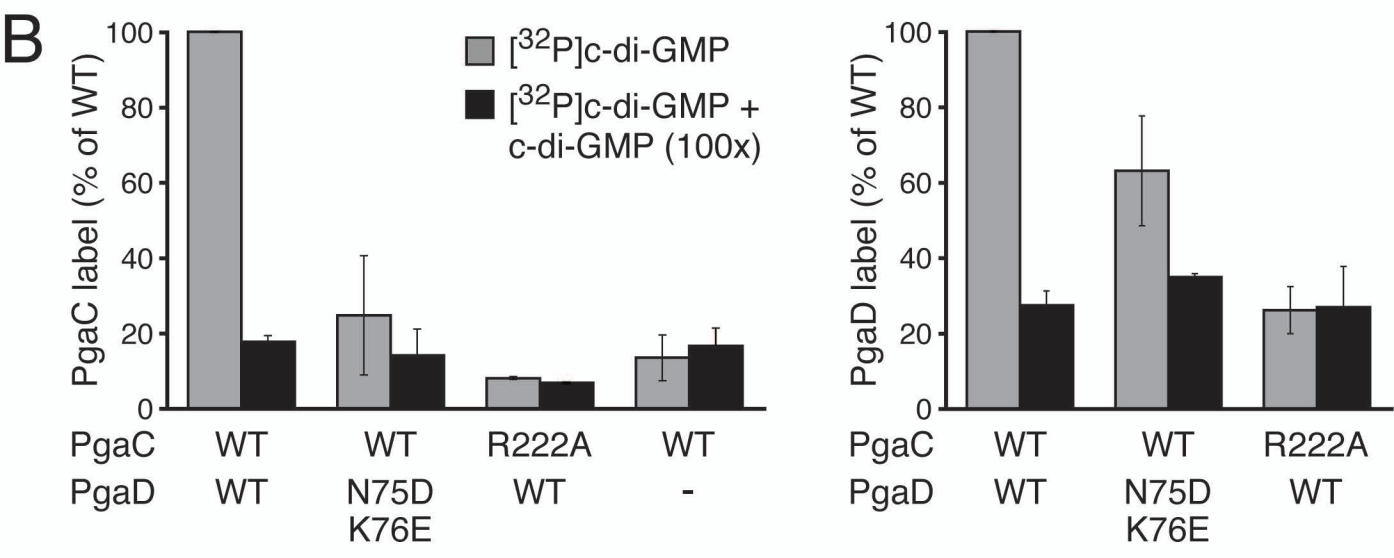
B
PgaC label (% of WT)
100
80
60
40
20
0
[32P]c-di-GMP
[32P]c-di-GMP + c-di-GMP (100x)
PgaC WT WT R222A WT
PgaD WT N75D K76E WT -
PgaD label (% of WT)
100
80
60
40
20
0
PgaC WT WT R222A
PgaD WT N75D K76E WT

Steiner *et al.* Figure 8

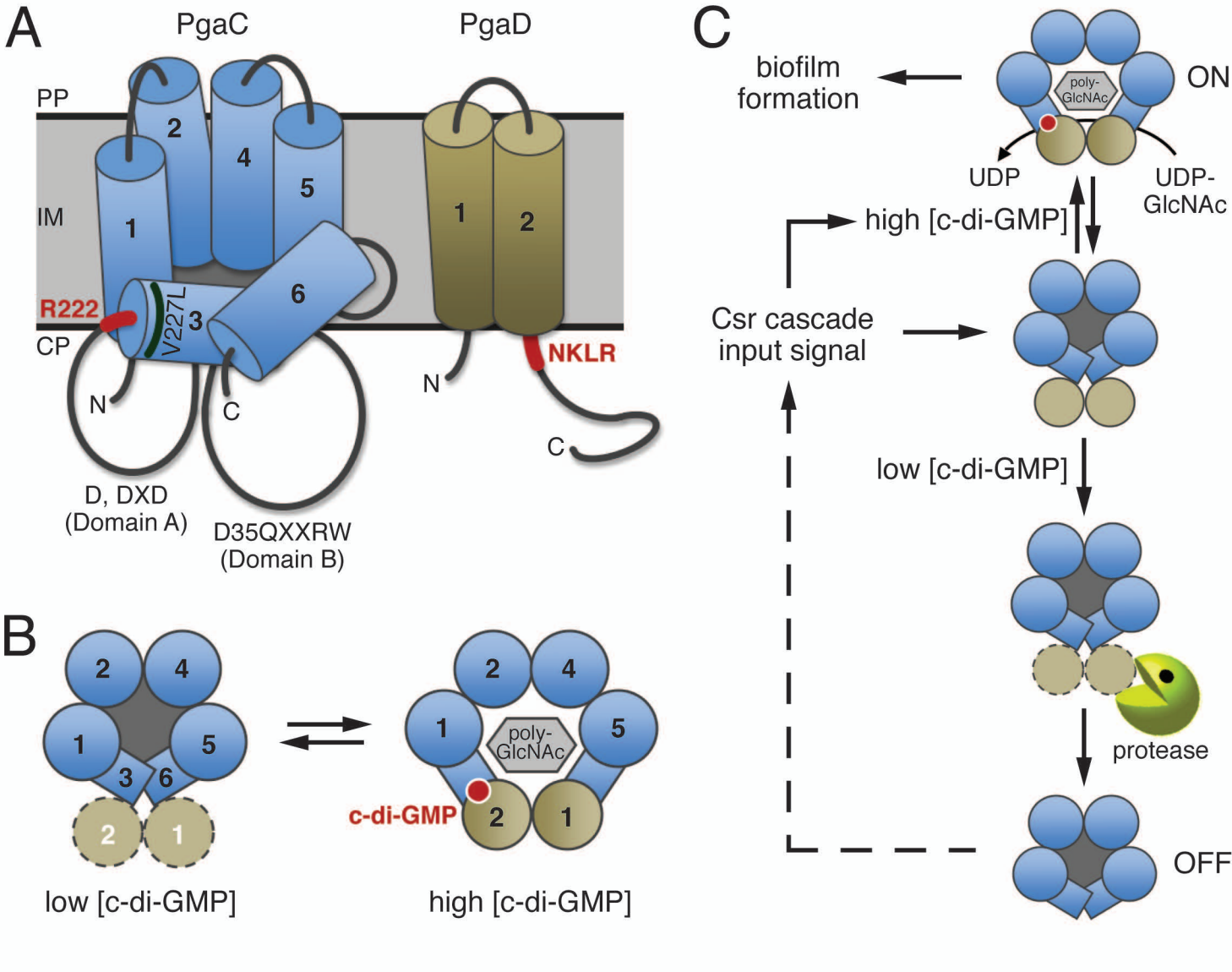

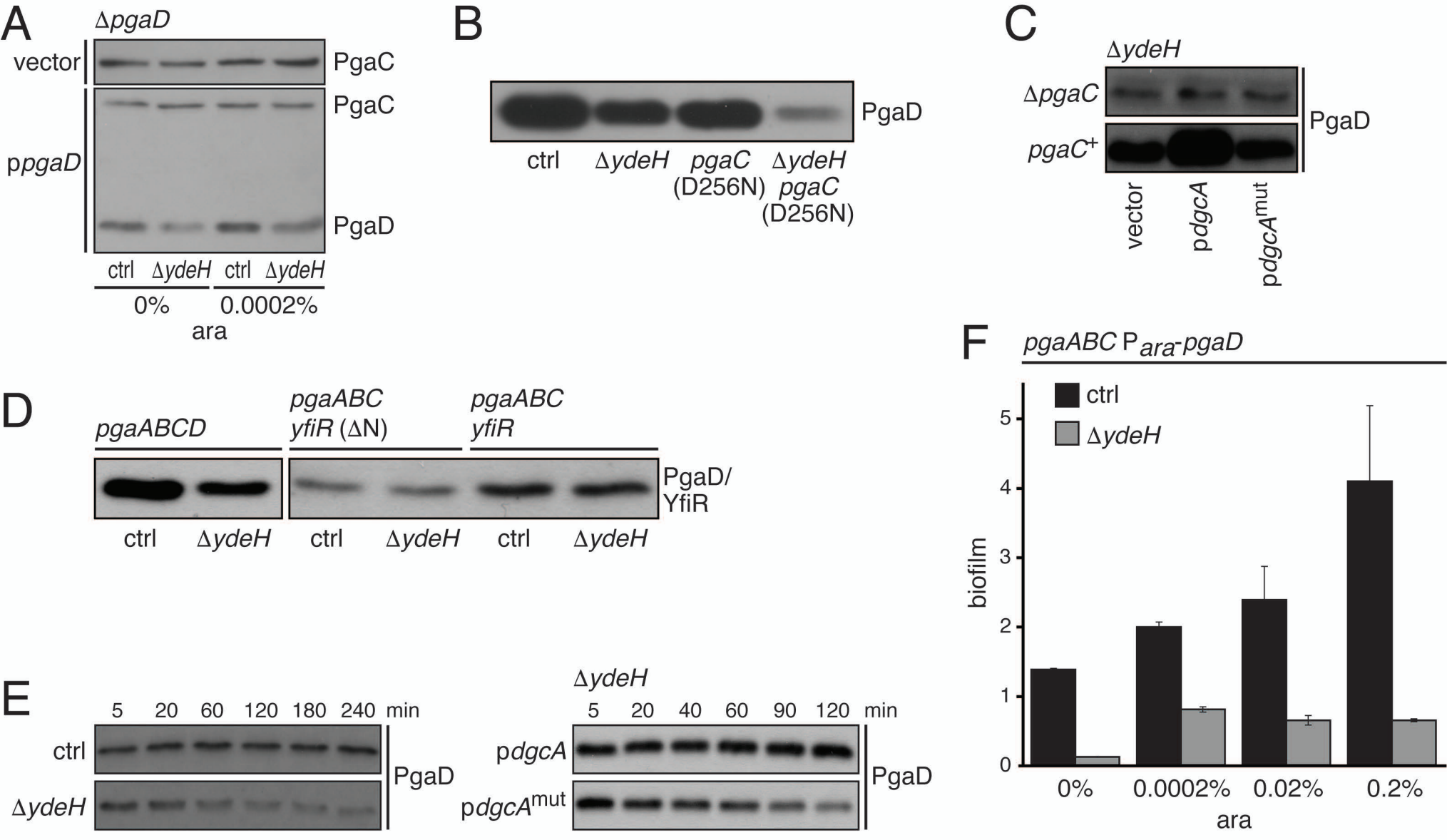
A
ΔpgaD
vector
ppgaD
PgaC
PgaC
PgaD
ctrl
ΔydeH
ctrl
ΔydeH
0%
0.0002%
ara
B
PgaD
ctrl
ΔydeH
pgaC (D256N)
ΔydeH pgaC (D256N)
C
ΔydeH
ΔpgaC
pgaC+
PgaD
vector
pdgcA
pdgcAmut
D
pgaABCD
pgaABC yfiR (ΔN)
pgaABC yfiR
PgaD/ YfiR
ctrl
ΔydeH
ctrl
ΔydeH
ctrl
ΔydeH
E
5 20 60 120 180 240 min
ctrl
ΔydeH
PgaD
ΔydeH
5 20 40 60 90 120 min
pdgcA
pdgcAmut
PgaD
F
pgaABC Para-pgaD
ctrl
ΔydeH
biofilm
0
1
2
3
4
5
0%
0.0002%
0.02%
0.2%
ara

Steiner *et al*. Supplementary Figure 2

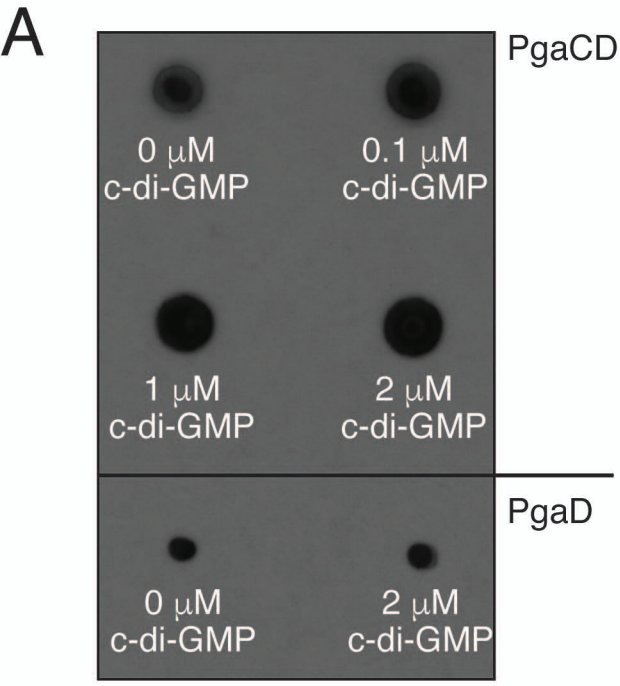

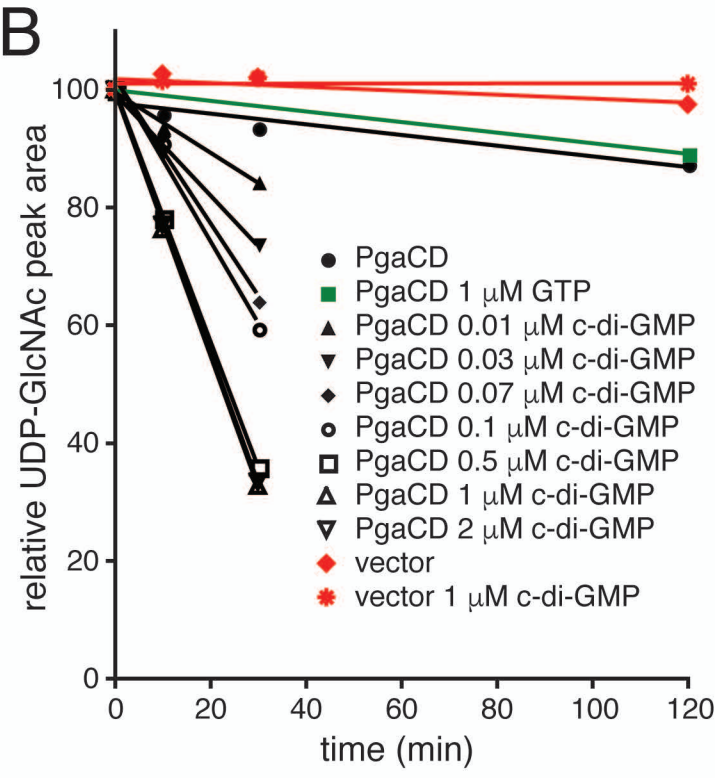

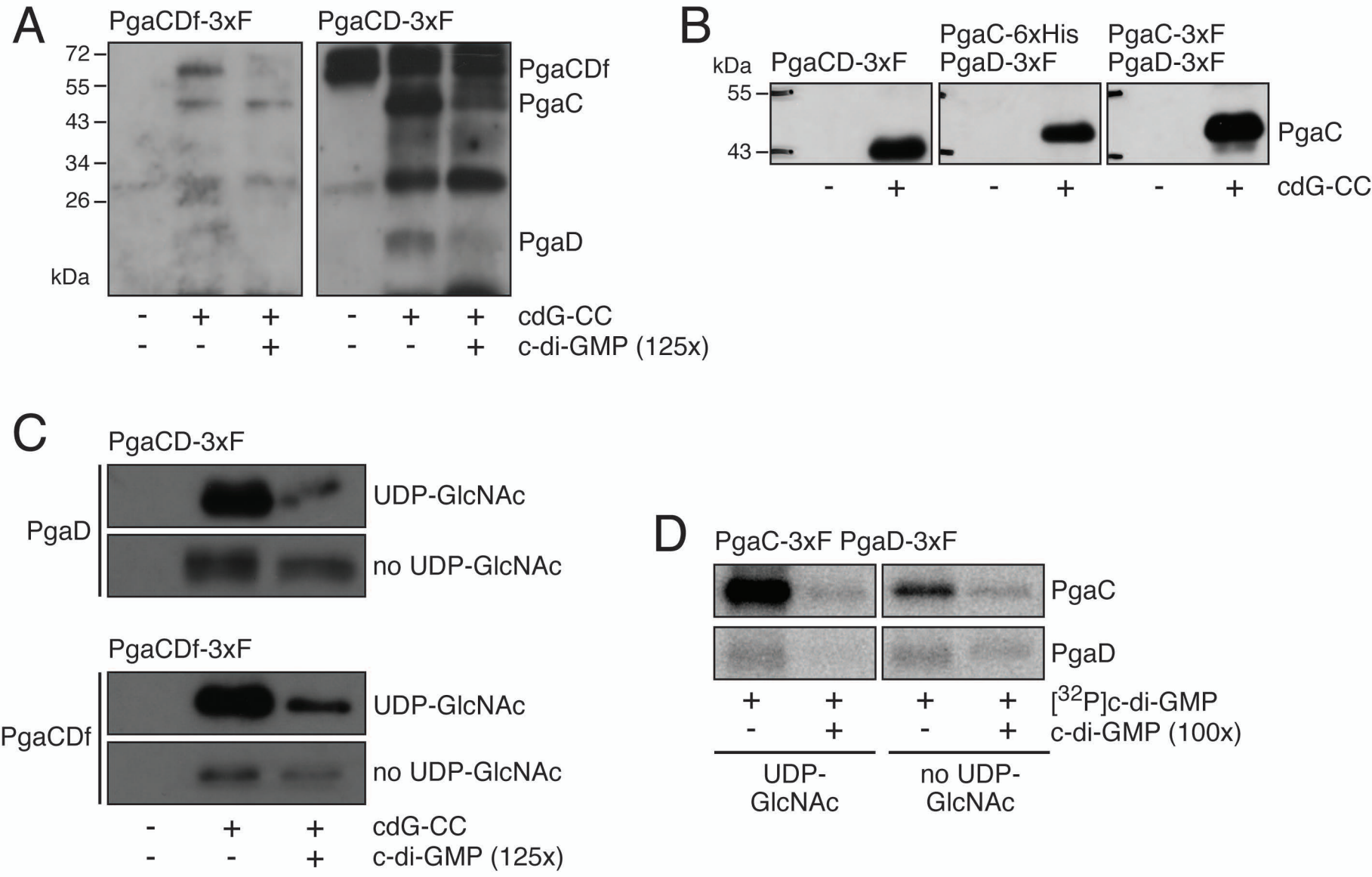
A
PgaCDf-3xF
PgaCD-3xF
72
55
43
34
26
kDa
PgaCDf
PgaC
PgaD
- + + - + + cdG-CC
- - + - - + c-di-GMP (125x)
B
kDa
PgaCD-3xF
PgaC-6xHis PgaD-3xF
PgaC-3xF PgaD-3xF
55
43
PgaC
- + - + - + cdG-CC
C
PgaCD-3xF
PgaD
UDP-GlcNAc
no UDP-GlcNAc
PgaCDf-3xF
PgaCDf
UDP-GlcNAc
no UDP-GlcNAc
- + + cdG-CC
- - + c-di-GMP (125x)
D
PgaC-3xF PgaD-3xF
PgaC
PgaD
+ + + + [32P]c-di-GMP
- + - + c-di-GMP (100x)
UDP-GlcNAc
no UDP-GlcNAc

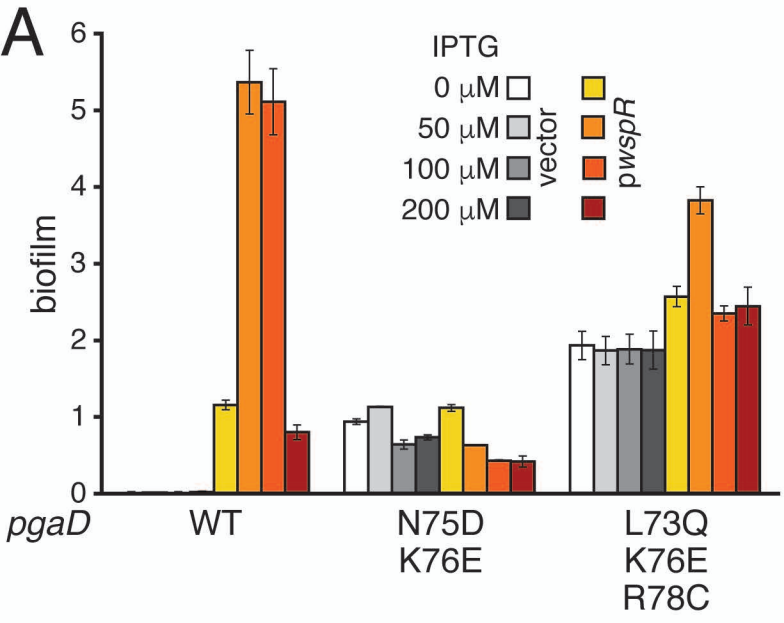
A
biofilm
IPTG
0 μM
50 μM
100 μM
200 μM
vector
pwspR
pgaD
WT
N75D
K76E
L73Q
K76E
R78C

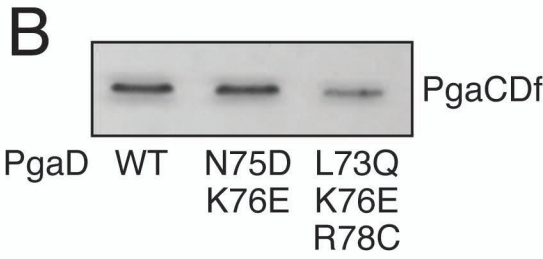
B
PgaCDf
PgaD
WT
N75D
K76E
L73Q
K76E
R78C

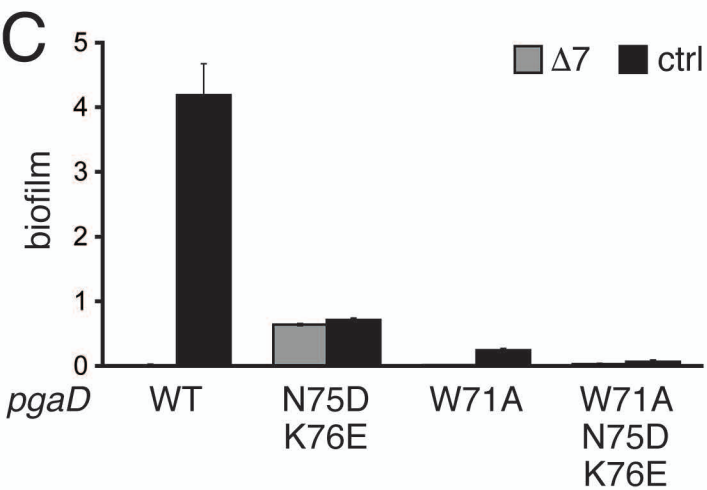
C
biofilm
Δ7
ctrl
pgaD
WT
N75D
K76E
W71A
W71A
N75D
K76E

Steiner *et al*. Supplementary Figure 5

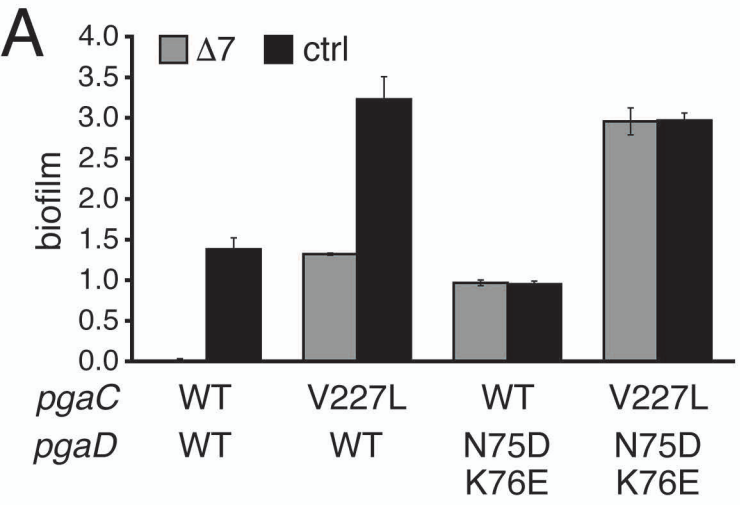

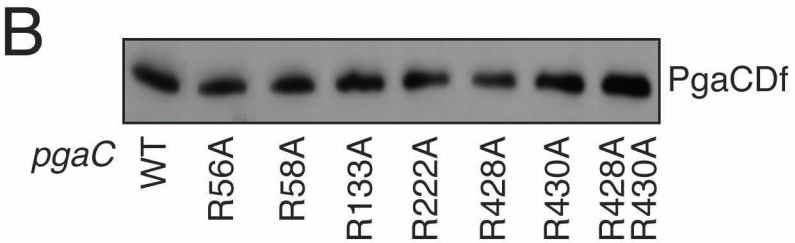

W60R

TMD1

TMD2

D

D X D

R222A

V227L

S260T

MAD3

D

Q X X R W

TMD4

TMD5

MAD6

a	*Escherichia coli* K-12 MG1655	c-di-GMP
b	*Yersinia pestis* (HmsR)	signaling
c	*Pseudomonas fluorescens*	
d	*Shigella flexneri*	
e	*Escherichia fergusonii*	
f	*Acinetobacter baumannii*	
g	*Acinetobacter junii*	
h	*Actinobacillus pleuropneumoniae*	no c-di-GMP
i	*Aggregatibacter actinomycetemcomitans*	signaling
j	*Mannheimia succiniciproducens*	
k	*Haemophilus parainfluenzae*	

Supplementary Table 1 Strains and plasmids used in this study.

E. coli strains

Name	Relevant genotype	Description/comments	Source/reference
MG1655	wild-type	*E. coli* K-12 wild-type	(Blattner *et al*, 1997)
AB330	DY330 λ cI^{857} Δ(*cro-bioA*)	temperature sensitive, λRED system	(Yu *et al*, 2000)
AB958	*csrA*::Tn*5*Δ(*kan*)::*Frt*	ancestor of most strains used in this study	(Boehm *et al*, 2009)
AB959	*csrA*::Tn*5*Δ(*kan*)::*Frt* Δ*ydeH*::*Frt*		(Boehm *et al*, 2009)
AB1062	*csrA*::Tn*5*Δ(*kan*)::*Frt pgaD*-3xFlag-*kan*		(Boehm *et al*, 2009)
AB1063	*csrA*::Tn*5*Δ(*kan*)::*Frt* Δ*ydeH*::*Frt pgaD*-3xFlag-*kan*		(Boehm *et al*, 2009)
AB1094	*csrA*::Tn*5*Δ(*kan*)::*Frt Frt-araC-araBfpgaA* (tl.) *pgaD*-3xFlag-*Frt* Δ*araBC*::*Frt*	translational *araB-pgaA* fusion, *kan-araC*-P$_{ara}$ amplified from TB55	This work
AB1313 *	*csrA*::Tn*5*Δ(*kan*)::*Frt* Δ*ydeH*::*Frt* Δ*yegE*::*Frt* Δ*ycdT*::*Frt* Δ*yfiN*::*Frt* Δ*yhjK*::*Frt* Δ*ydaM*::*Frt* Δ*yneF*::*Frt* *	c-di-GMP^{low} Δ7 mutant	This work
AB1412	*csrA*::Tn*5*Δ(*kan*)::*Frt pgaC*-3xFlag Δ*pgaD*::*Frt*		This work
AB1413	*csrA*::Tn*5*Δ(*kan*)::*Frt pgaC*-3xFlag Δ*pgaD*::*Frt* Δ*ydeH*::*Frt*		This work
AB1416	*csrA*::Tn*5*Δ(*kan*)::*Frt Frt-araC-araBfpgaA* (tl.) *pgaD*-3xFlag-*Frt* Δ*araBC*::*Frt* Δ*ydeH*::*Frt*	translational *araB-pgaA* fusion, *kan-araC*-P$_{ara}$ amplified from TB55	This work
AB1417	*csrA*::Tn*5*Δ(*kan*)::*Frt pgaA*-3xFlag Δ*pgaBCD*::*kan*		(Boehm *et al*, 2009)
AB1418	*csrA*::Tn*5*Δ(*kan*)::*Frt pgaB*-3xFlag Δ*pgaCD*::*kan*		This work
AB1419	*csrA*::Tn*5*Δ(*kan*)::*Frt* Δ*ydeH*::*Frt pgaA*-3xFlag Δ*pgaBCD*::*kan*		(Boehm *et al*, 2009)
AB1420	*csrA*::Tn*5*Δ(*kan*)::*Frt* Δ*ydeH*::*Frt pgaB*-3xFlag Δ*pgaCD*::*kan*		This work
AB1433	*csrA*::Tn*5*Δ(*kan*)::*Frt* Δ*araBC*::*Frt Frt-kan-Frt-araC-araBfpgaA*-3xFlag (tl.) Δ*pgaBCD*::*cat*	translational *araB-pgaA* fusion, *kan-araC*-P$_{ara}$ amplified from TB55	This work
AB1434	*csrA*::Tn*5*Δ(*kan*)::*Frt* Δ*araBC*::*Frt* Frt-*kan-Frt-araC-araBfpgaAB*-3xFlag (tl.) Δ*pgaCD*::*cat*	translational *araB-pgaA* fusion, *kan-araC*-P$_{ara}$ amplified from TB55	This work
AB1435	*csrA*::Tn*5*Δ(*kan*)::*Frt* Δ*araBC*::*Frt Frt-kan-Frt-araC-araBfpgaABC*-3xFlag (tl.) Δ*pgaD*::*cat*	translational *araB-pgaA* fusion, *kan-araC*-P$_{ara}$ amplified from TB55	This work
AB1514	*csrA*::Tn*5*Δ(*kan*)::*Frt* Δ*ydeH*::Frt Δ*araBC*::*Frt Frt-kan-Frt-araC-araBfpgaA*-3xFlag (tl.) Δ*pgaBCD*::*cat*	translational *araB-pgaA* fusion, *kan-araC*-P$_{ara}$ amplified from TB55	This work
AB1515	*csrA*::Tn*5*Δ(*kan*)::*Frt* Δ*ydeH*::*Frt* Δ*araBC*::*Frt Frt-kan-Frt-araC-araBfpgaAB*-3xFlag (tl.) Δ*pgaCD*::*cat*	translational *araB-pgaA* fusion, *kan-araC*-P$_{ara}$ amplified from TB55	This work
AB1516	*csrA*::Tn*5*Δ(*kan*)::*Frt* Δ*ydeH*::*Frt* Δ*araBC*::*Frt Frt-kan-Frt-araC-araBfpgaABC*-3xFlag (tl.) Δ*pgaD*::*cat*	translational *araB-pgaA* fusion, *kan-araC*-P$_{ara}$ amplified from TB55	This work
AB1537	*csrA*::Tn*5*Δ(*kan*)::*Frt* Δ*pgaD*::*yfiR* (ΔN)-3xFlag-*kan*	*yfiR* (ΔN)-3xF amplified from pMR20-*yfiR*-M2 (Malone *et al*, 2010)	This work
AB1538	*csrA*::Tn*5*Δ(*kan*)::*Frt* Δ*pgaD*::*yfiR*-3xFlag-*kan*	*yfiR*-3xF amplified from pMR20-*yfiR*-M2 (Malone *et al*, 2010)	This work
AB1539	*csrA*::Tn*5*Δ(*kan*)::*Frt* Δ*ydeH*::*Frt* Δ*pgaD*::*yfiR* (ΔN)-3xFlag-*kan*	*yfiR* (ΔN)-3xF amplified from pMR20-*yfiR*-M2 (Malone *et al*, 2010)	This work
AB1540	*csrA*::Tn*5*Δ(*kan*)::*Frt* Δ*ydeH*::*Frt* Δ*pgaD*::*yfiR*-3xFlag-*kan*	*yfiR*-3xF amplified from pMR20-*yfiR*-M2 (Malone *et al*, 2010)	This work
AB1569	*csrA*::Tn*5*Δ(*kan*)::*Frt* Δ*pgaD*::*Frt*		This work
AB1570	*csrA*::Tn*5*Δ(*kan*)::*Frt* Δ*ydeH*::*Frt* Δ*pgaD*::*Frt*		This work
AB1572	*csrA*::Tn*5*Δ(*kan*)::*Frt* Δ*araBC*::*Frt Frt-kan-Frt-araC-araBfpgaD* (tl.)	translational *araB-pgaD* fusion, *kan-araC*-P$_{ara}$ amplified from TB55	This work
AB1574	*csrA*::Tn*5*Δ(*kan*)::*Frt* Δ*ydeH*::*Frt* Δ*araBC*::*Frt Frt-kan-Frt-araC-araBfpgaD* (tl.)	translational *araB-pgaD* fusion, *kan-araC*-P$_{ara}$ amplified from TB55	This work

Steiner *et al*. Supplementary Table 1

Name	Relevant genotype	Description/comments	Source/reference
AB1638	*csrA*::Tn*5*Δ(*kan*)::*Frt* Δ*araBC*::*Frt* Δ*pgaABCD*::*Frt*	strain used for overexpressions (c-di-GMP binding assays)	This work
AB1645	*csrA*::Tn*5*Δ(*kan*)::*Frt* Δ*pgaABC*::*Frt pgaD*-3xFlag-*kan*		This work
AB1647	*csrA*::Tn*5*Δ(*kan*)::*Frt* Δ*ydeH*::*Frt* Δ*pgaABC*::*Frt pgaD*-3xFlag-*kan*		This work
AB1747	*csrA*::Tn*5*Δ(*kan*)::*Frt* Δ*pgaC*::*Frt pgaD*-3xFlag-*kan*		This work
AB1768	Δ*cyaA*::*Frt*	standard strain for bacterial two-hybrid analysis	This work
AB1775	*csrA*::Tn*5*Δ(*kan*)::*Frt* Δ*araBC*::*Frt Frt-kan-Frt-araC-araB*f*pgaA* (tl.)	translational *araB-pgaA* fusion, *kan-araC*-P_{ara} amplified from TB55	This work
AB1776	*csrA*::Tn*5*Δ(*kan*)::*Frt* Δ*araBC*::*Frt Frt-kan-Frt-araC-araB*f*pgaA* (tl.) Δ*pgaC*::*Frt*	translational *araB-pgaA* fusion, *kan-araC*-P_{ara} amplified from TB55	This work
AB1777	*csrA*::Tn*5*Δ(*kan*)::*Frt* Δ*araBC*::*Frt Frt-kan-Frt-araC-araB*f*pgaA* (tl.) Δ*pgaD*::*Frt*	translational *araB-pgaA* fusion, *kan-araC*-P_{ara} amplified from TB55	This work
AB1789	*csrA*::Tn*5*Δ(*kan*)::*Frt pgaC* (D256N) *pgaD*-3xFlag-*Frt*	PgaC active site mutant, secondary mutation Q70R present in *pgaC*	This work
AB1803	*csrA*::Tn*5*Δ(*kan*)::*Frt pgaC* (D256N) *pgaD*-3xFlag-*Frt* Δ*ydeH*::*Frt*	PgaC active site mutant, secondary mutation Q70R present in *pgaC*	This work
AB1880	*csrA*::Tn*5*Δ(*kan*)::*Frt* Δ*cyaA*::*Frt pgaC-T18* Δ*pgaD*::Δ*bla*::*Frt* Δ*araBC*::*Frt* Δ*cpdA*::*Frt*	strain for bacterial two-hybrid, *T18* amplified from pUT18	This work
AB1885	*csrA*::Tn*5*Δ(*kan*)::*Frt* Δ*ydeH*::*Frt* Δ*yegE*::*Frt* Δ*ycdT*::*Frt* Δ*yfiN*::*Frt* Δ*yhjK*::*Frt* Δ*ydaM*::*Frt* Δ*yneF*::*Frt pgaD*-3xFlag-*kan*	c-di-GMP^{low} Δ7 mutant	This work
AB1936	*csrA*::Tn*5*Δ(*kan*)::*Frt* Δ*cyaA*::*Frt pgaC-T18* Δ*pgaD*::Δ*bla*::*Frt* Δ*cpdA*::*Frt*	strain for bacterial two-hybrid, *T18* amplified from pUT18	This work
AB1937	*csrA*::Tn*5*Δ(*kan*)::*Frt* Δ*ydeH*::*Frt* Δ*cyaA*::*Frt pgaC-T18* Δ*pgaD*::Δ*bla*::*Frt* Δ*cpdA*::*Frt*	strain for bacterial two-hybrid, *T18* amplified from pUT18	This work
AB2020	*csrA*::Tn*5*Δ(*kan*)::*Frt* Δ*pgaC*::*kan*		This work
AB2021	*csrA*::Tn*5*Δ(*kan*)::*Frt* Δ*ydeH*::*Frt* Δ*yegE*::*Frt* Δ*ycdT*::*Frt* Δ*yfiN*::*Frt* Δ*yhjK*::*Frt* Δ*ydaM*::*Frt* Δ*yneF*::*Frt* Δ*pgaC*::*kan*	constitutive mutant screening strain, c-di-GMP^{low} Δ7 mutant	This work
AB2022	*csrA*::Tn*5*Δ(*kan*)::*Frt* Δ*ydeH*::*Frt* Δ*yegE*::*Frt* Δ*ycdT*::*Frt* Δ*yfiN*::*Frt* Δ*yhjK*::*Frt* Δ*ydaM*::*Frt* Δ*yneF*::*Frt pgaB*-3xFlag Δ*pgaCD*::*kan*	constitutive mutant screening strain, c-di-GMP^{low} Δ7 mutant	This work
AB2043	*csrA*::Tn*5*Δ(*kan*)::*Frt* Δ*ydeH*::*Frt* Δ*yegE*::*Frt* Δ*ycdT*::*Frt* Δ*yfiN*::*Frt* Δ*yhjK*::*Frt* Δ*ydaM*::*Frt* Δ*yneF*::*Frt* Δ*pgaABCD*::*Frt* Δ*araBC*::*Frt*	strain used for overexpressions (c-di-GMP binding assays; GT activity assays), c-di-GMP^{low} Δ7 mutant	This work
AB2134	*csrA*::Tn*5*Δ(*kan*)::*Frt* Δ*ydeH*::*Frt* Δ*yegE*::*Frt* Δ*ycdT*::*Frt* Δ*yfiN*::*Frt* Δ*yhjK*::*Frt* Δ*ydaM*::*Frt* Δ*yneF*::*Frt* Δ*pgaD*::*kan*	constitutive mutant screening strain, c-di-GMP^{low} Δ7 mutant	This work
AB2135	*csrA*::Tn*5*Δ(*kan*)::*Frt* Δ*pgaD*::*kan*		This work
AB2165	*csrA*::Tn*5*Δ(*kan*)::*Frt* Δ*ydeH*::*Frt* Δ*yegE*::*Frt* Δ*ycdT*::*Frt* Δ*yfiN*::*Frt* Δ*yhjK*::*Frt* Δ*ydaM*::*Frt* Δ*yneF*::*Frt pgaC-T18* Δ*pgaD*::*bla* Δ*cyaA*::*Frt* Δ*cpdA*::*Frt*	strain for bacterial two-hybrid, *T18* amplified from pUT18	This work
AB2166	*csrA*::Tn*5*Δ(*kan*)::*Frt* Δ*ydeH*::*Frt* Δ*yegE*::*Frt* Δ*ycdT*::*Frt* Δ*yfiN*::*Frt* Δ*yhjK*::*Frt* Δ*ydaM*::*Frt* Δ*yneF*::*Frt pgaC*::*Frt pgaD*-3xFlag-*kan*	c-di-GMP^{low} Δ7 mutant	This work
AB2297	*csrA*::Tn*5*Δ(*kan*)::*Frt* Δ*ydeH*::*Frt* Δ*ycdT*::*Frt*		This work
AB2306	*csrA*::Tn*5*Δ(*kan*)::*Frt* Δ*yegE*::*Frt* Δ*ycdT*::*Frt* Δ*yfiN*::*Frt* Δ*yhjK*::*Frt* Δ*ydaM*::*Frt* Δ*yneF*::*kan*		This work
TB55	DY329 P_{minC}<>(*kan-araC*-P_{ara})	used for amplification of *kan-araC*-P_{ara} to construct translational *araB* fusions	(Bernhardt and de Boer, 2004)
DH5α	(F-) F` *endA*1 *hsdR*17 (rK-mK plus) *glnV*44 *thi*1 *recA*1 *gyr* Δ(Nal^{R}) *relA*1 Δ(*lacIZYA-argF*)U169 *deoR* (Φ80d*lac* Δ(*lacZ*) M15)	used for general cloning purposes	(Woodcock *et al*, 1989)

Steiner *et al*. Supplementary Table 1

Plasmids

Name	Relevant genotype	Description/comments	Source/reference
pKD3	Amp^R Cm^R	Frt-flanked Cm^R gene, for chromosomal gene disruptions	(Datsenko and Wanner, 2000)
pKD4	Amp^R Km^R	Frt-flanked Km^R gene, for chromosomal gene disruptions	(Datsenko and Wanner, 2000)
pKD46	λRED$^+$ Amp^R	arabinose-inducible expression of λRED system	(Datsenko and Wanner, 2000)
pCP20	FLP$^+$ Amp^R Cm^R	temperature-sensitive replication and thermal induction of FLP synthesis	(Cherepanov and Wackernagel, 1995)
pSUB11	3xFlag Km^R	3xFlag-tagging of chromosomal genes	(Uzzau *et al*, 2001)
pME6032	*lacI*^{q}-P_{tac} (Tet^R)	IPTG-inducible expression vector, used as vector control for p*wspR*	(Heeb *et al*, 2002)
p*wspR*	pME6010::*wspR* (Tet^R)	*wspR* from *P. aeruginosa*	(Malone *et al*, 2007)
pUT18	P_{lac} T18 Amp^R	pUC19 derivative, used for fusions to the N-terminus of the T18 fragment of CyaA	(Karimova *et al*, 1998)
pUT18C	P_{lac} T18 Amp^R	pUC19 derivative, used for fusions to the C-terminus of the T18 fragment of CyaA	(Karimova *et al*, 1998)
pKT25	P_{lac} T25 Km^R	pSU40 derivative, used for fusions to the C-terminus of the T25 fragment of CyaA	(Karimova *et al*, 1998)
pUT18C-zip	pUT18C::*zip*	pUT18C derivative with T18 fused to leucine zipper of GCN4	(Karimova *et al*, 1998)
pKT25-zip	pKT25::*zip*	pKT25 derivative with T25 fused to leucine zipper of GCN4	(Karimova *et al*, 1998)
p18	pUT18::*pgaC*		This work
pF	pUT18::*pgaC* (G63-R318)		This work
pD	pUT18::*pgaC* (E384-G441)		This work
pΔGT	pUT18::*pgaC* (ΔP75-K314)		This work
pV	pUT18C::*pgaC* (G63-R318)		This work
pX	pUT18C::*pgaC* (E384-G441)		This work
pG2	pKT25::*pgaD*		This work
pB	pKT25::*pgaD* (Y74-A137)		This work
pBAD18	*araC*$^+$ *bla*$^+$ P_{araBAD} (Amp^R)	arabinose-inducible expression vector	(Guzman *et al*, 1995)
pAB551	pBAD18::*dgcA*	*dgcA* (cc3285) from *C. crescentus*	(Boehm *et al*, 2009)
pAC551	pBAD18::*dgcA* (D164N)	active site mutant of *dgcA* (cc3285) from *C. crescentus*	This work
p5a	pBAD18::*pgaC*		This work
p6a	pBAD18::*pgaC*-3xF	*pgaC*-3xF amplified from AB1412	This work
pins1	pBAD18::*pgaD*-3xF	*pgaD*-3xF amplified from AB1062	This work
pCD-3xF	pBAD18::*pgaC pgaD*-3xF	*pgaCD*-3xF amplified from AB1062	This work
pCDfusion	pBAD18::*pgaCD*f-3xF	PgaCD fusion protein, C-terminus of PgaC fused to N-terminus of PgaD	This work
p2-3xF	pBAD18::*pgaC*-3xF *pgaD*-3xF		This work
p2-3xF-DE	pBAD18::*pgaC*-3xF *pgaD*-3xF (N75D, K76E)		This work
p2-3xF-R222	pBAD18::*pgaC*-3xF (R222A) *pgaD*-3xF		This work
pC-His-D-3xF	pBAD18::*pgaC*-6xHis *pgaD*-3xF		This work
pD-P92	pBAD18::*pgaD* (-P92 trunc.)	truncated PgaD, last amino acid P92	This work
pD-Q80	pBAD18::*pgaD* (-Q80 trunc.)	truncated PgaD, last amino acid Q80	This work

Steiner *et al*. Supplementary Table 1

Name	Relevant genotype	Description/comments	Source/reference
pD-R78	pBAD18::*pgaD* (-R78 trunc.)	truncated PgaD, last amino acid R78	This work
pD-K76	pBAD18::*pgaD* (-K76 trunc.)	truncated PgaD, last amino acid K76	This work
pCL2	pBAD18::*pgaC* (W60R)	isolated constitutive allele	This work
pCL3	pBAD18::*pgaC* (S7P, M44T, W60R)	isolated constitutive allele	This work
pCL5	pBAD18::*pgaC* (R222A)		This work
pCL6	pBAD18::*pgaC* (D256N)	*pgaC* active site mutant	This work
pCL7	pBAD18::*pgaC*-3xF (S7P)		This work
pCL8	pBAD18::*pgaC*-3xF (M44T)		This work
pCL9	pBAD18::*pgaC*-3xF (W60R)		This work
pCL10	pBAD18::*pgaC*-3xF (S7P, W60R)		This work
pCL11	pBAD18::*pgaC*-3xF (M44T, W60R)		This work
pCL12	pBAD18::*pgaC*-3xF (S7P, M44T, W60R)		This work
pCL13	pBAD18::*pgaC*-3xF (V227L)		This work
pCL20	pBAD18::*pgaD*-3xF (L73Q, K76E, R78C)	isolated constitutive allele	This work
pCL22	pBAD18::*pgaD*-3xF (K76E)	isolated constitutive allele	This work
pCL23	pBAD18::*pgaD*-3xF (N75D)		This work
pCL25	pBAD18::*pgaD*-3xF (N75D, K76E)	isolated constitutive allele	This work
pCL28	pBAD18::*pgaD*-3xF (L73Q)		This work
pCL29	pBAD18::*pgaD*-3xF (R78C)		This work
pCL30	pBAD18::*pgaD*-3xF (L73Q, K76E)		This work
pCL31	pBAD18::*pgaD*-3xF (K76E, R78C)		This work
pCL32	pBAD18::*pgaD*-3xF (W71A)		This work
pCL33	pBAD18::*pgaD*-3xF (Y74A)		This work
pCL34	pBAD18::*pgaD*-3xF (W71A, N75D, K76E)		This work
pCL42	pBAD18::*pgaC* (V227L) *pgaD*-3xF		This work
pCL43	pBAD18::*pgaC pgaD*-3xF (N75D, K76E)		This work
pCL44	pBAD18::*pgaC* (V227L) *pgaD*-3xF (N75D, K76E)		This work
pCL45	pBAD18::*pgaC* (R222A) *pgaD*-3xF		This work
pCL46	pBAD18::*pgaC* (R222A) *pgaD*-3xF (N75D, K76E)		This work
pCL54	pBAD18::*pgaC* (V227L) *D*f-3xF	PgaCD fusion protein, C-terminus of PgaC fused to N-terminus of PgaD	This work
pCL55	pBAD18::*pgaCD* (N75D, K76E) f-3xF	PgaCD fusion protein, C-terminus of PgaC fused to N-terminus of PgaD	This work
pCL56	pBAD18::*pgaCD* (L73Q, K76E, R78C) f-3xF	PgaCD fusion protein, C-terminus of PgaC fused to N-terminus of PgaD	This work
pCL58	pBAD18::*pgaCD* (W71A) f-3xF	PgaCD fusion protein, C-terminus of PgaC fused to N-terminus of PgaD	This work
pCL59	pBAD18::*pgaC* (R56A) *D*f-3xF	PgaCD fusion protein, C-terminus of PgaC fused to N-terminus of PgaD	This work
pCL60	pBAD18::*pgaC* (R58A) *D*f-3xF	PgaCD fusion protein, C-terminus of PgaC fused to N-terminus of PgaD	This work
pCL61	pBAD18::*pgaC* (R56A, R58A) *D*f-3xF	PgaCD fusion protein, C-terminus of PgaC fused to N-terminus of PgaD	This work
pCL62	pBAD18::*pgaC* (R133A) *D*f-3xF	PgaCD fusion protein, C-terminus of PgaC fused to N-terminus of PgaD	This work

Name	Relevant genotype	Description/comments	Source/reference
pCL63	pBAD18::*pgaC* (R222A) *D*f-3xF	PgaCD fusion protein, C-terminus of PgaC fused to N-terminus of PgaD	This work
pCL64	pBAD18::*pgaC* (R428A) *D*f-3xF	PgaCD fusion protein, C-terminus of PgaC fused to N-terminus of PgaD	This work
pCL65	pBAD18::*pgaC* (R430A) *D*f-3xF	PgaCD fusion protein, C-terminus of PgaC fused to N-terminus of PgaD	This work
pCL66	pBAD18::*pgaC* (R428A, R430A) *D*f-3xF	PgaCD fusion protein, C-terminus of PgaC fused to N-terminus of PgaD	This work
pCL68	pBAD18::*pgaC* (R198D) *D*f-3xF	PgaCD fusion protein, C-terminus of PgaC fused to N-terminus of PgaD	This work
pCL72	pBAD18::*pgaC* (V227L)	isolated constitutive allele	This work

* AB1313, the ancestor of all *csrA* Δ7 c-di-GMP^{low} strains, harbors an approximately 11 kb deletion of the entire region between *ydeH* and *yneF*. The deletion, which arose during the last gene deletion event and the subsequent Flp recombinase-mediated marker removal, does not account for the biofilm formation phenotype of AB1313, since the immediate ancestor of AB1313 (*yneF*$^{+}$, *csrA* Δ6, no deletion) showed comparable c-di-GMP- and/or constitutive allele-mediated biofilm formation (data not shown). Detailed protocols of strain and plasmid constructions are available on request.

Supplementary Table 2 Overview of bacterial two-hybrid analysis.

T18-	expression	-T18	expression	T25-	expression	interaction
PgaC (G63-R318)	yes	-	-	PgaD	n/a	no
PgaC (E384-G441)	no	-	-	PgaD	n/a	no
-	-	PgaC	n/a	PgaD	n/a	YES
-	-	PgaC	n/a	PgaD (Y74-A137)	no	no
-	-	PgaC (G63-R318)	yes	PgaD	n/a	no
-	-	PgaC (E384-G441)	no	PgaD	n/a	no
-	-	PgaC (ΔP75-K314)	n/a	PgaD	n/a	no

T18-X on pUT18C, X-T18 on pUT18, T25-X on pKT25. Some constructs were 1xFlag-tagged to check for expression by immunoblot. n/a = expression not tested. See also Supplementary Figure 6 and Figure 5A.

Supplementary Table 3 Isolated constitutive mutations in *pgaC* and *pgaD*.

pgaC		*pgaD*		*pgaCD*	
DNA	AA	DNA	AA	DNA	AA
t178a	**W60R**	a226g	**K76E**	g509a	**R170H** (*pgaC*)
		a421g	**K141E** *	g679a	**V227I** (*pgaC*)
t19c	**S7P**			t1001a	**F334Y** (*pgaC*)
t131c	**M44T**	a97g	**I33V**		
t168c	silent	a223g	**N75D**	c600g	silent (*pgaC*)
t178a	**W60R**	a226g	**K76E**	a151g	**R51G** (*pgaD*)
		a300g	silent		
g679t	**V227L**			g779c	**S260T** (*pgaC*)
t696c	silent	a226g	**K76E**		
a903g	silent				
a1254t	silent	a223g	**N75D**		
		a226g	**K76E**		
a512g	**D171G**				
g679t	**V227L**	t218a	**L73Q**		
a1021g	**I341V**	a226g	**K76E**		
		c232t	**R78C**		
t378c	silent				
g679c	**V227L**				
g1173c	silent				
a7g	**N3D**				
g779c	**S260T**				
t1047a	silent				

In the first two columns, either *pgaC* or *pgaD* was mutagenized. The third column shows alleles isolated when *pgaC* and *pgaD* were simultaneously mutagenized. Mutations on the DNA level as well as resulting amino acid exchanges are indicated. * Mutation lies within the C-terminal 3xFlag tag of *pgaD*.